NASA TECHNICAL MEMORANDUM

NASA TM X-72012

COPY NO.

NASA TM X-72012

DESIGN FEATURES AND OPERATIONAL CHARACTERISTICS OF THE LANGLEY PILOT TRANSONIC CRYOGENIC TUNNEL

By Robert A. Kilgore

September 23, 1974

NATIONAL AERONAUTICS AND SPACE ADMINISTRATION
LANGLEY RESEARCH CENTER, HAMPTON, VIRGINIA 23665

1. Report No.	2. Government Accession No.	3. Recipient's Catalog No.
NASA TM X-72012		

4. Title and Subtitle	5. Report Date
Design Features and Operational Characteristics of the Langley Pilot Transonic Cryogenic Tunnel	September 23, 1974
	6. Performing Organization Code

7. Author(s)	8. Performing Organization Report No.
Robert A. Kilgore	
	10. Work Unit No.

9. Performing Organization Name and Address	11. Contract or Grant No.
NASA Langley Research Center Hampton, Virginia 23665	
	13. Type of Report and Period Covered
12 Sponsoring Agency Name and Address	High-Number TM X
National Aeronautics and Space Administration Washington, D. C. 20546	14. Sponsoring Agency Code

15 Supplementary Notes

Interim release of material, to be combined with additional material and converted to a formal publication by December 31, 1975.

16 Abstract

Experience with the fan-driven transonic cryogenic tunnel indicates that such a tunnel presents no unusual design difficulties and is simple to operate. In addition, purging, cooldown, and warmup times have been found to be acceptable and can be predicted with good accuracy. Experience over a wide range of operating conditions indicates that cooling with liquid nitrogen is practical at the power levels required for transonic testing and that good temperature distributions are obtained by using a simple nitrogen injection system.

17. Key Words (Suggested by Author(s)) (STAR category underlined)	18. Distribution Statement
Facilities, research and support Reynolds number, cryogenic, wind tunnel	Unclassified-Unlimited

19. Security Classif. (of this report)	20. Security Classif. (of this page)	21. No. of Pages	22. Price*
Unclassified	Unclassified	58	$3.75

*Available from { The National Technical Information Service, Springfield, Virginia 22151
STIF/NASA Scientific and Technical Information Facility, P O. Box 33, College Park, MD 20740

NATIONAL AERONAUTICS AND SPACE ADMINISTRATION

DESIGN FEATURES AND OPERATIONAL CHARACTERISTICS OF THE LANGLEY PILOT TRANSONIC CRYOGENIC TUNNEL

By Robert A. Kilgore
Langley Research Center
Hampton, Virginia

SUMMARY

A theoretical investigation by Smelt in 1945 indicated that the use of air at cryogenic temperatures would permit large reductions of wind-tunnel size and power requirements in comparison with a wind tunnel operated at normal temperature and at the same pressure, Mach number, and Reynolds number. Lack of suitable cooling techniques and suitable structural materials precluded application of this cryogenic wind-tunnel concept at the time of Smelt's work. Because of the recent advances in cryogenic engineering and structural materials and the current interest, both in this country and in Europe, in the development of high Reynolds number transonic tunnels, a program has been initiated recently at the NASA Langley Research Center to extend the analyses of Smelt and to study the feasibility of the cryogenic wind-tunnel concept.

Following the completion of a low-speed cryogenic tunnel experiment in the summer of 1972 it was decided to extend the experimental work to transonic speeds. Design of a transonic tunnel began in December of 1972 with initial operation in September of 1973.

Experience with the fan-driven transonic cryogenic tunnel indicates that

such a tunnel presents no unusual design difficulties and is simple to operate. In addition, purging, cooldown, and warmup times have been found to be acceptable and can be predicted with good accuracy. Experience over a wide range of operating conditions indicates that cooling with liquid nitrogen is practical at the power levels required for transonic testing and that good temperature distributions are obtained by using a simple nitrogen injection system.

INTRODUCTION

A theoretical investigation by Smelt in reference 1 in 1945 indicated that the use of air at temperatures in the cryogenic range, that is, below about 172 K (-150°F), would permit large reductions of wind-tunnel size and power requirements in comparison with a wind tunnel operated at normal temperature and at the same pressure, Mach number, and Reynolds number. The lack of a practical means of cooling a wind-tunnel to cryogenic temperatures and the unavailability of suitable structural materials precluded application of this cryogenic wind-tunnel concept at the time of Smelt's work.

The first practical application of the cryogenic concept was a low temperature test rig for centrifugal compressors as reported by Rush in reference 2. The test rig consisted of a single-stage compressor pumping air through a closed circuit containing an air-liquid nitrogen heat exchanger which cooled the air to about 125 K. By operating at very low temperatures, dynamic similarity was achieved with a substantial reduction in both rotational speed and the power required to drive the compressor. In this application of the cryogenic concept, the main interest was in the reduction of rotational speed and the attendant reduction in impeller loading which allowed development tests to be conducted with impellers of easily machined materials.

In the autumn of 1971, while studying ways of increasing test Reynolds number of the small tunnels for which magnetic suspension and balance systems had been developed, it was decided to investigate the use of cryogenic test temperatures. Theoretically, such an approach is ideally suited for this application since for a given size tunnel operating at constant stagnation pressure there is realized a large increase in Reynolds number with no increase in dynamic pressure or model loads. Further study quickly indicated that the

advances which have been made in recent years in the field of cryogenic engineering and structural materials have been such that a cryogenic wind-tunnel appears practical and should be given serious consideration.

Following a theoretical investigation started in October 1971 and aimed at extending the analysis of Smelt, an experimental program was initiated with the objective of verifying some of the theoretical predictions and to expose and solve the practical problems of using a cryogenic wind-tunnel. The experimental program consisted of building and operating two fan-driven cryogenic wind-tunnels, both of which were cooled to cryogenic temperatures by injecting liquid nitrogen (LN_2) directly into the tunnel circuit. The first was a low-speed atmospheric tunnel. The results of the theoretical investigation and the low-speed study have been reported in references 3 and 4.

Following the completion of the low-speed cryogenic tunnel experiment in the summer of 1972, it became apparent that the concept was a serious contender for the new high Reynolds number transonic tunnels being contemplated both in the U.S. and Europe and it was decided to extend the experimental work to transonic speeds. After some deliberation on how best to proceed, it was decided that a continuous-flow fan-driven pressure tunnel would provide the most flexible tool for the exploration of this application of cryogenic principles. The purpose of the transonic cryogenic pressure tunnel is to demonstrate in compressible flow that cryogenic gaseous nitrogen is a valid transonic test gas; to demonstrate at high power levels the method of cooling; to determine any limitations imposed by liquefaction of the test gas; to verify engineering concepts with a realistic tunnel configuration; and to provide operational experience. Design of the transonic tunnel began in December of 1972 with initial operation in September of 1973.

A brief description of the Langley Pilot Transonic Cryogenic Tunnel and some of the preliminary experimental results have been published in references 5 and 6. The purpose of this paper is to describe in more detail the design and operational characteristics of the tunnel and ancillary equipment and to present the results of preliminary calibration tests.

SYMBOLS

A	test-section area, m
L_p	sound pressure level, dB (reference 20 $\mu N/m^2$)
M	Mach number
p	pressure, atm (1 atm = 101.3×10^3 kN/m^2)
q	free-stream dynamic pressure, N/m^2
R	Reynolds number
T	temperature, K (K = °C + 273.15)
V	free-stream velocity, m/s
η	tunnel power factor
σ	standard deviation

Subscripts:

t	stagnation conditions
L	local conditions
∞	free-stream conditions

DESCRIPTION OF THE TRANSONIC TUNNEL AND ANCILLARY EQUIPMENT

The Langley Pilot Transonic Cryogenic Tunnel has been constructed at the NASA Langley Research Center and is a single-return fan-driven tunnel with a slotted octagonal test section 34.3 cm (13.5 in.) across flats. The tunnel can be operated at Mach numbers from near 0.05 to about 1.3 at stagnation pressures from slightly greater than 1 atmosphere to 5 atmospheres over a temperature range from 340 K to about 77 K (152° F to about -320° F). The ranges of pressure and temperature provide the opportunity of investigating Reynolds number effects by temperature and pressure independently over almost a 5 to 1 range of Reynolds number.

A sketch of the tunnel circuit is shown in figure 1 and a photograph of the tunnel taken during assembly is shown in figure 2. Some details of the mechanical aspects of the pilot cryogenic tunnel have been reported in reference 7. A more detailed description of the tunnel is given in the sections which follow.

Materials of Construction

The tunnel pressure shell is constructed of 0.635 and 1.270 cm (0.25 and 0.50 in.) thick plates of 6061-T6 aluminum alloy. The flanges used to join the various sections of the tunnel were machined from plates of this same material. The bolts for the flanges are made from 2024-T4 aluminum alloy. These particular aluminum alloys were selected because they have good mechanical characteristics at cryogenic as well as ambient temperatures and could easily be fabricated using equipment and techniques available at Langley.

The flange joints, depending upon size, are sealed with either a flat gasket or a teflon coated hollow metal "o"-ring. Several different types of

seals were tested at pressure under both ambient and cryogenic conditions to determine their suitability for use with the cryogenic tunnel. Because of its reusability, the flat gasket seal, made from a mixture of teflon resin and pulverized glass fiber, w selected as the best seal overall. However, since gasket material was not available in widths sufficient to make gaskets for the largest flanges, a teflon coated hollow "o"-ring of 321 stainless steel is used at each of the three largest flanges. Subsequent experience has shown that completely satisfactory large gaskets can be made from relatively small pieces of the flat gasket material if they are joined with dovetail joints. Sketches of typical flange joints are shown in figure 3.

Tunnel Support System

The tunnel supports shown in figure 1 are constructed in two parts. The upper portion of each support, which might be cooled to very low temperatures, is made from 347 stainless steel. The lower portion, which is never subjected to low temperatures, is made of A-36 carbon steel.

The 3200 kg (7050 lbm) tunnel is mounted on the four "A"-frame support stands shown in figure 1, one of which is a "tunnel anchor" support designed so that the center of the fan hub keeps a fixed position relative to the drive motor. Thermal expansion and contraction of the tunnel results in a change in overall tunnel length of about 4.0 cm (1.57 in.) between extremes in operating temperature. Sliding pads at each of the tunnel support attachments allow free thermal expansion or contraction of the tunnel structure. The sliding surfaces consist of 2.54 cm (1 in.) thick teflon sheets placed between the support attachments on the tunnel and the stainless steel blocks mounted on the upper

portion of the carbon steel "A"-frame stands. Vertical and lateral movement at each joint is constrained by bolts passing through the tunnel support attachment and the teflon sheet into the "A"-frame. The tunnel support attachments are slotted in the longitudinal direction to allow free longitudinal expansion or contraction of the tunnel. A sketch of the tunnel anchor support is shown in figure 4.

The object of the anchor support is to hold the centerline of the tunnel at this support in a fixed position relative to the ground in the presence of relatively large amounts of thermal expansion. The undersides of all of the tunnel support attachments, including those at the anchor point, are on the horizontal plane through the axis of the return leg of the tunnel. With symmetrical expansion, the tunnel centerline is held at a fixed height above the ground. A fork on the tunnel underside at the anchor point, shown on figure 4, additionally prevents lateral or axial movement of the tunnel at this station. In this way the axis at the anchor point is fixed relative to the ground and the tunnel expands and contracts symmetrically about this point on the axis. Since the fan and tunnel are both manufactured from aluminum, thermal expansion does not materially affect the tip clearance of the fan or generate any misalignment between the axis of the fan and the externally mounted drive motor. This support scheme has proved to be entirely adequate and no problems have been encountered.

Thermal Insulation

Thermal insulation for most of the tunnel circuit consists of 12.7 cm (5 in.) of blown urethane foam applied to the outside of the tunnel structure with

a glass fiber reinforced polyester vapor barrier on the outside. A sketch showing a typical section of the thermal insulation and the method used to insulate the flanges is presented in figure 5. As can be seen in figure 5, the urethane foam is not bonded directly to the aluminum tunnel but rather is separated from the wall by a shear layer consisting of two layers of fiberglass cloth. This allows the differential expansion between the aluminum and urethane foam to take place without causing the foam to fracture. In addition, the insulation is applied in two layers separated by a layer of fiberglass cloth. Again, the purpose of the fiberglass shear layer within the insulation is to allow differential expansion to take place within the urethane foam insulation itself without fracture. This insulation has proved adequate and keeps the outside of the tunnel warm and dry under all operating conditions even during periods of high humidity.

Viewing and Lighting Ports

Seven ports are provided to allow illumination and visual inspection of the interior of the tunnel in the plenum and test-section areas and the nitrogen injection regions. A sketch of one of the ports showing details of construction is shown in figure 6. Each of the ports consists of a 3.56 cm (1.4 in.) diameter glass window which is designed to take the maximum differential pressure of 4 atmospheres at cryogenic temperatures. To provide protection against possible window failure and to provide thermal insulation, two 0.953 cm (0.375 in.) thick sheets of clear polycarbonate resin plastic, separated by air gaps, are fitted securely over each glass window. Should these sheets of plastic also fail following failure of the glass window, additional protection is provided by a third sheet of plastic fitted as a blast shield to standoff supports on

the port assembly such that the shield is not subjected to the tunnel pressure. The tunnel is capable of operating indefinitely at cryogenic temperatures and therefore it is necessary to purge with ambient temperature dry nitrogen between the layers of plastic in order to prevent dew or frost from forming on the outer surface.

It should be noted that there is no fundamental reason for using such small diameter ports. The small size of the present ports was chosen to limit to a harmless level the pressure rise which would occur in the building which houses the tunnel in the event of failure of a glass window with the tunnel operating at a maximum pressure and minimum temperature.

Initially, the inside of the tunnel was illuminated by directing the collimated output of three small incandescent lamps into the tunnel through three of the ports. With this system, a layer of 0.635 cm (0.25 in.) thick heat-absorbing glass was placed between the light source and the port to prevent any differential heating of the glass window. Recently, however, a simple yet very effective light source has been placed inside the plenum chamber which provides illumination for both the test section and plenum region. The new light source consists of two 12-volt automobile stop-light bulbs mounted in an evacuated plastic box which in turn is fastened to one of the test-section walls.

Drive-Fan System

The tunnel has a fixed geometry drive-fan system which consists of 7 pre-rotation vanes and a 12-bladed fan followed by 15 anti-swirl vanes. The photograph presented as figure 7 is a view looking upstream at the fan and shows the section of the tunnel just downstream of the fan-section which

contains the nacelle. The hollow nacelle was cast from 6061-T6 aluminum alloy and then machined on the outside to provide an aerodynamically smooth surface.

The drive fan is powered by a 2.2 MW (3000 hp) water-cooled synchronous motor with variable-frequency speed control. The motor, which is external to the tunnel, is capable of operating at speeds from 600 rpm to slightly less than 7200 rpm. However, at present, operation of the fan/motor system is restricted to speeds below 6200 rpm due to the excitation of resonance in the drive shaft between the motor and the fan at this speed.

Return-Leg Diffuser and Turning Vanes

The return-leg diffuser section is shown in the photograph presented as figure 8. Shown in this photograph are two of the liquid nitrogen injection spray bars and two of the ports used for illuminating and viewing the spray bars. As can be seen, no attempt was made to fair the spray bars to reduce their drag. Also shown in figure 8 is the tunnel section containing the 3rd and 4th corners. The turning-vane design shown here is typical of all four corners which have the same 15-vane arithmetic progression spacing design which has been used successfully in the 8ft x 8ft Supersonic Tunnel at the Royal Aircraft Establishment, Bedford, and which is to be used in the 5 meter Low Speed Tunnel now under construction at RAE, Farnborough.

Screen Section

The screen section is shown in the photograph presented as figure 9. The screen design requirement was to provide a turbulence level in the test section of 0.1 percent. Each of the three screens is made from 0.0165 cm (0.0065 in.)

diameter monel wire woven with approximately 16 openings per centimeter (40 openings per inch). Also shown in figure 9 is the temperature survey rig. This rig is located upstream of the screens and comprises eight arms and a center-support ring which are aerodynamically faired to reduce the possibility of the wake from the rig adversely affecting the flow quality in the test section. (The thermocouple elements were covered with tape when the photograph was taken.)

Contraction Section

The contraction section of the transonic tunnel has a 12 to 1 contraction ratio. The contraction section was designed with a smooth distribution of wall curvature with low curvature at both the entrance and exit regions in order to avoid, if possible, boundary layer separation in these two critical regions. In consideration of good lateral velocity distribution, the test-section end of the contraction section was favored in the design to provide sufficient length for very low curvature in this region. The contraction section, shown during construction in the photograph presented as figure 10, is designed so that the transition from the circular cross-section at the downstream end of the screens to the octogonal cross-section of the up-stream end of the test section follows exactly the prescribed longitudinal variation in cross-sectional area. Also, the design is such that the streamlines near the walls cross only one weld in the critical high velocity region. The circumferential weld was hand finished so that the entire inner surface of the contraction section is aerodynamically smooth. The variation of contraction section area with longitudinal station is given in table I.

Test Section

The slotted-wall octagonal test section is 34.32 cm (13.511 in.) across flats and 85.73 cm (33.75 in.) long. The entire test section, including the longitudinal variation of open area, is modeled after the test section evolved for the Langley 16-Foot Transonic Tunnel before that tunnel was equipped with a plenum air removal system. Provision is made for changing the slot configuration and adjusting the wall divergence over a range from zero to 30 minutes of arc. Adjustable re-entry flaps at the downstream end of the slots allow control over the amount of diffuser suction. Some details of test-section design and the initial geometrical settings are shown on figures 11, 12, and 13 and in table II. A photograph of the test-section is presented in figure 14. With the initial test-section configuration the maximum test-section Mach number is 1.06. In order to operate above $M_\infty = 1.06$, the tunnel must be operated at pressures sufficiently high to allow gas to be exhausted from the plenum. This is achieved by passing gas from the plenum chamber through pressure regulating valves directly to the atmosphere. Under these conditions, test-section Mach numbers up to about 1.3 can be obtained.

Liquid Nitrogen System

A schematic drawing of the liquid nitrogen system is shown in figure 15. Liquid nitrogen is stored at atmospheric pressure in two vacuum insulated tanks having a total capacity of about 30,000 liters (8,000 U.S. gallons). When the tunnel is being operated at less than about 2.5 atmospheres absolute pressure the liquid can be supplied to the tunnel simply by pressurizing the supply tank with the pressurizing coil shown in figure 15. The liquid nitrogen pump must

be used whenever the tunnel is operated at high pressures. When the pump is used, the supply tank is pressurized to about 1.7 atmospheres absolute pressure in order to maintain sufficient net positive suction head at the pump inlet to prevent cavitation. The pump has a capacity of about 500 liters per minute (150 U.S. gallons per minute) with a delivery pressure of 9.3 atmospheres absolute, and is driven by a 22.4 kW (30 hp) constant-speed electric motor.

When the pump is used, the liquid nitrogen supply pressure is set and held constant by the pressure control valve, shown in figure 15, which regulates the amount of liquid returned to the storage tank through the pressure-control return line.

The flow rate of liquid nitrogen into the tunnel circuit is regulated by pneumatically operated control valves located outside the tunnel at each of the three injection stations. These valves, which may be used either singly or in combination, can be controlled either manually or automatically. A helium filled constant-volume bulb thermometer located in the settling chamber serves as the temperature sensing element when the valves are being controlled automatically.

Since the transonic tunnel operates over wide ranges of pressure and Mach number it is necessary to allow for a wide range of liquid nitrogen flow rate. This is accomplished by designing the spray bar at each of the injection stations to cover a limited range of flow rates by the proper selection of the number as well as the size of the nozzles used on each spray bar. By operating various combinations of the three spray bars and by changing the liquid nitrogen supply pressure, liquid nitrogen flow rates from 1 to 400 liters per minute (0.25 to 107 U.S. liquid gallons per minute) are realized.

Originally, ten nozzles having small orifice diameters were used on each

of the spray bars at injection stations 2 and 3 shown in figure 15. These nozzles were prone to become blocked with foreign matter inadvertently (but perhaps inevitably) left in the liquid nitrogen supply system. The twenty original nozzles were replaced with eight nozzles having larger orifice diameters.

The two types of nozzles currently in use are shown in figure 16. Both types are commercial nozzles designed to give a full-cone spray pattern and fine spray particles over a wide range of spraying pressure. Sketches in figure 17 show the type and number of nozzles currently used at each of the injection stations. The flow capacity as a function of the differential pressure across the nozzle is also tabulated on figure 17.

In its present configuration, the liquid nitrogen system has two principal deficiencies. The first of these is the rather lengthy time required to cool the LN_2 supply pipes. The minimum time required to cool the pipe between the LN_2 pump and the injection stations is determined by the rate at which the gas generated during the cooldown process can be vented to the atmosphere through the tunnel exhaust system without damage to turbine flow meters located in the liquid nitrogen supply pipes at each injection station. The minimum supply pipe cooldown time with the present system is about 30 minutes. A recirculating loop supply system would greatly reduce this cooldown time and also simplify the control of liquid nitrogen flow rate by eliminating boiling in the pipe during tunnel operation which is also a problem with the present system at very low flow rates.

The second deficiency arises from the fact that a completely pneumatic control system is used with the flow-rate control valves. Automatic control of flow rate and hence tunnel operating temperature is possible for only a very

limited range of conditions due to the very long response time of the pneumatic system.

Nitrogen Exhaust System

The system for exhausting gaseous nitrogen from the tunnel is shown schematically in figure 15. Tunnel total pressure is adjusted by means of pneumatically operated control valves in exhaust pipes leading to the atmosphere from the low-speed section of the tunnel. In order to minimize flow disturbance the exhaust pipes are taken from the low-speed section at 120° intervals just ahead of the 3rd set of turning vanes. The valves may be used either singly or in combination in order to provide fine control over a wide range of exhaust flow rates. A total pressure probe located downstream of the screens provides the reference pressure measurement when tunnel pressure is being controlled automatically.

As originally designed, the nitrogen exhaust from the tunnel vented directly to the atmosphere through pipes carried through the roof of the building housing the tunnel. A severe fogging problem existed with this original design during periods of high humidity and low wind speed. On several occasions it was necessary to suspend operations until there was a favorable change in the weather. A simple and completely effective solution to this problem has been found and consists of an exhaust driven ejector as shown in the sketch in figure 18. The low pressure ejector induces ambient air which dilutes and warms the cold nitrogen exhaust gas. The resulting foggy mixture is propelled high into the air and dissipates completely. No measurements have yet been made to determine the ratio of induced ambient air to exhaust nitrogen gas.

However, this simple exhaust ejector, which has an area ratio of about 5:1, induces sufficient ambient air and discharges the mixture so effectively that it has completely eliminated the fogging problem even under the most adverse weather conditions.

As noted in a preceding section, in order to operate above $M_\infty = 1.06$, the tunnel must be operated at pressures sufficiently high to allow gas to be exhausted from the plenum chamber to the atmosphere. Manually-controlled pneumatically-actuated valves in three pipes leading to the atmosphere from the plenum allow approximately one percent of the mass flow entering the test section to be exhausted when operating at $M_\infty = 1$ or greater. By using this method, test-section Mach numbers up to about 1.3 can be obtained. The plenum exhaust pipes lead from the plenum at 120° intervals through the upstream plenum wall. The control valves may be used either singly or in combination.

Instrumentation

In addition to special instrumentation required for test-section calibration and special aerodynamic tests, the tunnel is instrumented to measure temperatures and pressures around the circuit, dew point (or frost point) of the test gas, oxygen content of the test gas, pressure of the LN_2 supply, LN_2 flow rate, mass flow rate of the gas exhausting from the stilling section and the plenum chamber, changes in tunnel linear dimension with temperature, fan speed, and torque at the drive motor shaft.

OPERATING PROCEDURE

Many of the operating procedures developed for the low-speed cryogenic tunnel described in references 3 and 4 are being used with the transonic tunnel. However, since the transonic tunnel was designed and built purposely for cryogenic operation, the detailed procedures used for purging, cooldown, and running differ from those developed for the low-speed tunnel. A description of the operating procedures currently being used with the transonic tunnel is given in the sections which follow.

Purging

Any moisture in the tunnel circuit is removed by purging with nitrogen gas. With the present liquid nitrogen supply system, sufficient purging gas is generated during the cooldown of the supply pipes. The gas is injected into the tunnel circuit through the liquid-nitrogen injection nozzles. During the pre-run purge, the tunnel fan is used to maintain circulation and provide sufficient heat to maintain the stream and wall temperatures above the dew (or frost) point of the gas in the tunnel. The nitrogen exhaust system valves at the third turning vanes are used to keep the tunnel at about 1.2 atmospheres absolute pressure during the pre-run purge. At the end of the 30 minute period required to cool the liquid nitrogen supply pipes and get liquid nitrogen to the injection nozzles, the dew point is usually very close to the lower limit of measurement of the dew-point monitoring system. This limit is about 200 K (-80°F). Cooldown of the tunnel then commences.

Cooldown

Following the pre-run purging process, the stream and tunnel are cooled to the desired operating temperature by injecting liquid nitrogen into the tunnel at the rate of about 75 liters per minute (about 20 U.S. gallons per minute) using injection station number 3 shown on figure 15. The total pressure of the gas in the settling chamber is held near 1.2 atmospheres absolute and the drive fan is operated at a constant speed of about 700 rpm during the cooldown process. This low speed provides the necessary circulation in the tunnel during the cooldown process without adding a significant amount of heat to the stream. Under these conditions, cooling the tunnel and the stream from 300 K (80°F) to 110 K (-262°F) requires, on average, 2450 liters (650 U.S. gallons) of LN_2 and takes about 30 minutes.

The required LN_2 flow rate as a function of cooldown time for cooling from 300 K to 110 K is shown on figure 19 for extremes in cooldown efficiency. These curves were calculated using the method of reference 8. Also shown on figure 19 is the experimental data quoted above which indicates that a 30 minute cooldown time is of average efficiency. Since, in general, slower cooldown rates are probably more efficient, increasing the cooldown time should tend to reduce the LN_2 requirement toward the lower value of 1725 liters which was used for the lower curve on figure 19.

Running

Following cooldown of the stream and tunnel to the desired operating temperature, test Mach number is set by adjustment of fan speed. The setting of Mach number is made while the tunnel is near 1.2 atmospheres absolute pressure.

A small computer automatically provides the operators with a continually updated display of Mach number based on the ratio of total pressure measured downstream of the screens to static pressure measured in the plenum. Once Mach number is set, the desired operating total pressure is obtained by adjustment of nitrogen-exhaust control valves. While adjusting total pressure, the liquid nitrogen flow rate must also be adjusted to hold total temperature constant since the heat added by the fan is changing in direct proportion to pressure. Because of the interaction between the variables of fan speed, pressure, and LN_2 flow rate, and inadequacies in the automatic control systems, the tunnel controls are operated in a manual mode while setting the desired tunnel conditions. This procedure takes between 2 and 10 minutes with variation of operating pressure between 1.2 and 7 atmospheres absolute pressure. For the initial operation of this pilot cryogenic tunnel, there has been no effort made to improve on the performance of the control system. Improvements in the automatic control systems could undoubtedly be made which would reduce the time required to obtain the desired tunnel conditions.

The heat to be removed while running at constant test conditions consists of the heat conduction through the tunnel walls and the heat energy added to the tunnel circuit by the drive fan. The running LN_2 requirement has been calculated as a function of Mach number for the two extremes of total pressure for ambient and cryogenic operation. In calculating the heat conducted through the tunnel walls it was assumed that the inner surface of the tunnel was at a temperature equal to the stagnation temperature, T_t, that there was zero temperature gradient through the metal pressure shell, and that the outside surface temperature of the insulation was at 300 K (80°F). The portion of the main-drive fan power added to the stream as heat is assumed to be

$$\text{Power to stream} = qVA\eta$$

where q = free-stream dynamic pressure

V = free-stream velocity

A = test-section area

and η = tunnel power factor

The tunnel power factor, η, was based on values measured in several large transonic tunnels at the Langley Research Center. η was assumed to vary only with Mach number. The values of η which were used for these calculations are as follows:

M_∞	0.2 to 1.0	1.1	1.2
η	0.20	0.22	0.25

The estimated LN_2 requirements are shown on figure 20. It is interesting to note that at a given pressure the required nitrogen flow rate is not a strong function of temperature. This arises from the fact that while the power required to drive the tunnel decreases with decreasing temperature, the cooling capacity of the liquid nitrogen also decreases with decreasing temperature. Also shown are several measured values of LN_2 flow made during preliminary operation of the tunnel. Due to faults with the LN_2 supply system and flow-rate meters, there is considerable scatter in the experimental data. However, there is general agreement between the estimated and measured flow rates.

Warmup and Re-oxygenation

Following cryogenic operation, the tunnel is warmed, depressurized, and

calibration information but with particular emphasis being placed on identifying any problems related either to the method of cooling or to the wide range of operating temperature. The second type of experimental data is primarily aimed at determining the validity and the practicality of the cryogenic concept in compressible flow.

Some of the results obtained during the initial operation of the tunnel have been reported in references 5 and 6. Some of the results reported in references 5 and 6 along with additional results of the preliminary tunnel calibration are given in the sections which foll w.

Test-Section Mach Number Distribution

The test-section Mach number distribution has been determined over a wide range of test conditions. Static pressure orifices located along the tunnel wall and along a tunnel centerline probe were used to determine the static pressure distribution. A pitot tube located downstream of the screens is used to measure stagnation pressure. As noted in reference 4, for stagnation pressures up to about 5 atmospheres the isentropic expansion relations calculated from the real-gas properties of nitrogen differ by no more than about 0.4 percent (depending on test conditions) from the corresponding relations calculated from ideal diatomic gas properties and ideal gas equations. However, since the pressure measuring instrumentation being used is capable of resolving such differences, the appropriate real-gas relation is used to determine Mach number from the stagnation to static pressure ratio. The nominal test-section Mach number is calculated from the ratio of stagnation pressure measured just downstream of the screens to static pressure measured in the plenum chamber.

The initial calibration of the tunnel indicates nearly identical tunnel wall and tunnel centerline Mach number distributions for all test conditions. In addition, there are no detectable differences between Mach number distributions at ambient and cryogenic temperatures. An example of the tunnel wall and tunnel centerline Mach number distribution is shown in figure 22. Examples of the wall Mach number distribution over a range of Mach numbers is shown in figure 23. Since the purpose of these tests was only to validate the cryogenic concept, no attempt has yet been made to improve the distributions by changes to slot geometry, wall divergence, or re-entry flap position.

Transverse Temperature Distribution

Since the heat of compression of the fan is removed by spraying liquid nitrogen directly into the tunnel circuit, there was some concern about the uniformity of the resulting temperature distribution, particularly at the power levels required for transonic testing where the mass flow rate of liquid nitrogen is in the order of one percent of the test section mass flow rate. Therefore, it was decided to measure the transverse temperature distribution in the tunnel over a wide range of operating conditions in order to determine if there were any problems of uniformity of temperature distribution related to the method of cooling.

The temperature survey rig previously described and shown in the photograph presented as figure 9 was used to determine the transverse temperature distribution just ahead of the screens. Six examples of the transverse temperature distribution are shown in figure 24. These distributions, all obtained at a test-section free-stream Mach number of 0.85, are typical of the data

which have been obtained over the entire tunnel operating envelope. With each distribution is shown the mean value (arithmetic average) of temperature $\bar{T}_t$ and standard deviation (measure of dispersion around the mean) σ. As can be seen, there is a relatively uniform temperature distribution even at cryogenic temperatures where the tunnel is being operated within a few degrees of the test-section free-stream saturation conditions. It is expected that the screens and contraction section have a beneficial effect on temperature distribution such that the distribution in the test section is even more uniform than the distribution measured upstream of the screens.

Drive Power and Fan Speed

During the initial calibration and aerodynamic testing, measurements were to be made of both the drive-shaft torque and speed in order to allow comparisons to be made between predicted and measured values of drive power and fan speed with temperature, pressure, and Mach number. Problems with the torque measurements (unrelated to cryogenic operation) preclude for the present any accurate determination of drive power. However, based on power supplied to the drive motor, it appears that the drive power varies roughly as predicted by theory, namely, for constant pressure and Mach number, power varies directly with the speed of sound, that is, as $T^{0.5}$.

Satisfactory measurements were made of fan speed. On figure 25 is shown the theoretical variation of fan speed with temperature together with experimental values obtained at a test-section free-stream Mach number of 0.85 and at stagnation pressures of about 4.95 atmospheres. The Reynolds number in the test section varied from about 62×10^6 per meter (19×10^6 per foot) at the highest stagnation temperature, 326.7 K, to 327×10^6 per meter (99×10^6 per foot)

at the lowest temperature, 99.5 K. As can be seen, the fan speed actually decreases somewhat faster with decreasing temperature than predicted by the simple theory (speed $\propto T^{0.5}$), thus indicating perhaps a beneficial effect of the greatly increased Reynolds number on tunnel or fan efficiencies at the lower operating temperatures.

In an attempt to determine if the faster than predicted decrease in fan speed was indeed due to an increase in Reynolds number, additional fan speed data obtained at various Mach numbers was plotted as shown on figure 26. This figure covers only the limited cryogenic temperature range over which these particular tests were made. The fan speed at cryogenic temperature was referenced to the corresponding fan speed at ambient temperature for each Mach number. All of the ambient temperature fan speed data was obtained at stagnation pressures near 4.95 atmospheres. Two sets of data are shown at cryogenic temperatures. The fan speeds at cryogenic temperatures used to calculate the data shown by the flagged symbols were obtained at stagnation pressures near 1.2 atmospheres. The flagged symbols therefore represent nearly constant Reynolds number between the ambient and cryogenic temperature conditions. The fan speeds at cryogenic temperatures used to calculate the data shown by the unflagged symbols were obtained at stagnation pressures near 4.95 atmospheres. These data, therefore, represent a fourfold increase in Reynolds number between ambient and cryogenic temperature conditions.

As can be seen from the data, the relative fan speed for the constant Reynolds number conditions generally decreases with temperature slightly less than predicted by theory. However, the relative fan speed for the increased Reynolds number conditions decreases slightly faster than predicted by theory. Therefore, the faster decrease in fan speed with decreasing temperature shown

on figure 25 does in fact represent a true Reynolds number effect, indicating perhaps both improved fan performance and reduced skin friction around the tunnel circuit with increasing Reynolds number.

The data of figure 26 indicates that for constant Reynolds number conditions, fan speed in this particular tunnel varies approximately as $T^{0.487}$. For the constant pressure condition, where Reynolds number is increasing as temperature is reduced, fan speed varies approximately as $T^{0.543}$.

Test-Section Noise Measurements

The background noise in the test section is of concern since excessive noise levels can prevent the proper simulation of the unsteady aerodynamic parameters usually of interest in dynamic tests, and in addition, may affect certain static or steady-state parameters being measured. Because of the large reduction in both drive power and pressure as temperature is reduced, it was expected that background noise would be reduced when a given Reynolds number was obtained at cryogenic temperatures rather than at ambient temperature. Therefore noise measurements have been made in the test section over a range of test conditions in order to determine the effect of cryogenic operation on noise.

The test-section noise levels are presented in terms of the broadband (10 Hz to 20 kHz) sound pressure level, L_p, with the reference pressure taken to be 20 $\mu N/m^2$. The measurements were made during the testing of a two-dimensional airfoil at 3° incidence and $M_\infty = 0.80$ by a microphone which was mounted flush with the inner surface of the test section wall just above the airfoil. The noise levels are not strictly background noise because of the presence of the airfoil. The data, therefore, should not be used as an indication of the

minimum background noise in the test section but rather should be used comparatively to indicate the general effect of cryogenic operation on noise level. The sound pressure level data are presented in figure 27 as a function of Reynolds number per foot. Next to each plotted point are the corresponding values of stagnation pressure and temperature. As can be seen, at a constant Reynolds number of about 18×10^6, the combined effect of reducing temperature and pressure results in a reduction of the sound pressure level by 10 dB from the level measured at high pressure and ambient temperature. Data also was taken at a nearly constant pressure and shows Reynolds number increased by either a factor of 3 or 4.6, depending on the reduction in temperature, with only a 1 dB increase in the broadband sound pressure level.

Extensive analysis of the test-section noise data has not as yet been made. However, based on the limited amount of available data, significant reductions in noise level will be obtained at cryogenic temperature.

CONCLUSIONS

Many of the conclusions of the low-speed testing reported in references 3 and 4 were confirmed during the operation and testing in the transonic tunnel. Additional conclusions from the transonic tunnel are as follows:

1. A transonic cryogenic pressure tunnel is simple to operate.
2. Purging, cooldown, and warmup times are acceptable and can be predicted with good accuracy.
3. Liquid nitrogen requirements for cooldown and running can be predicted with good accuracy.
4. Cooling with liquid nitrogen is practical at the power levels required

for transonic testing. Test temperature is easily controlled and good temperature distribution obtained by using a simple nitrogen injection system.

5. Test-section noise level is reduced wher a given Reynolds number is obtained by operating at cryogenic temperatures.

REFERENCES

1. Smelt, R.: Power Economy in High Speed Wind Tunnels by Choice of Working Fluid and Temperature. Report No. Aero. 2081, Royal Aircraft Est. Farnborough, England, August 1945.

2. Rush, C. K.: A Low Temperature Centrifugal Compressor Test Rig. National Research Council of Canada, Ottawa Low Temperature Lab. MD-48; NRC-7776, November 1963.

3. Goodyer, M. J.; and Kilgore, R. A.: High-Reynolds-Number Cryogenic Wind Tunnel. AIAA Journal, Vol. 11, No. 5, May 1973, pp. 613-619. Presented as AIAA Paper No. 72-995 at the AIAA 7th Aerodynamic Testing Conference, Palo Alto, Calif., Sept. 13-15, 1972.

4. Kilgore, Robert A.; Goodyer, Michael J.; Adcock, Jerry B.; and Davenport, Edwin E. : The Cryogenic Wind Tunnel Concept for High Reynolds Number Testing. NASA TN-D 7762.

5. Kilgore, R. A.; Adcock, J. B.; and Ray, E. J.: Flight Simulation Characteristics of the Langley High Reynolds Number Cryogenic Transonic Tunnel. Preprint 74-80, Am. Inst. Aeron. and Astronaut., January 1974.

6. Ray, E. J.; Kilgore, R. A.; and Adcock, J. B.: Test Results from the Langley High Reynolds Number Cryogenic Transonic Tunnel. Preprint 74-631, Am. Inst. Aero. and Astronaut., July 1974.

7. Wilson, John F.; Ware, George D.; and Ramsy, James W., Jr.: Pilot Cryogenic Tunnel: Attachments, Seals, and Insulation. Paper presented at the ASCE National Structural Meeting, (Cincinnati, Ohio), April 22-26, 1974.

8. Jacobs, R. B.: Liquid Requirements for Cool-Down of Cryogenic Equipment. Advances in Cryogenic Engineering, Vol. 8, Plenum Press, 1963.

TABLE I

DESIGN DIMENSIONS OF THE TRANSONIC TUNNEL CONTRACTION SECTION

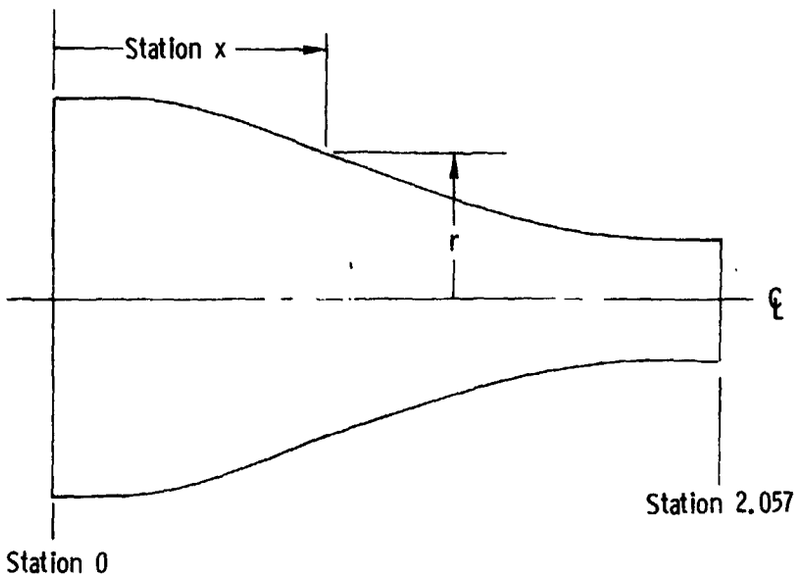

Longitudinal station x, m	Area, m^2	Equivalent-circle radius, r, m
0.000	1.167	0.610
.111	1.165	.609
.204	1.156	.607
.309	1.144	.603
.405	1.090	.589
.496	1.013	.568
.581	.922	.541
.657	.831	.514
.730	.744	.486
.802	.661	.459
.873	.583	.431
.941	.511	.403
1.009	.445	.377
1.078	.386	.351

Longitudinal station x, m	Area, m^2	Equivalent-circle radius, r, m
1.143	0.344	0.326
1.210	.288	.303
1.278	.248	.281
1.345	.213	.260
1.414	.183	.241
1.481	.158	.225
1.550	.140	.211
1.620	.126	.200
1.691	.115	.192
1.763	.108	.185
1.834	.102	.181
1.908	.100	.178
1.982	.098	.177
2.057	.098	.176

TABLE II

TRANSONIC TUNNEL TEST-SECTION SLOT GEOMETRY

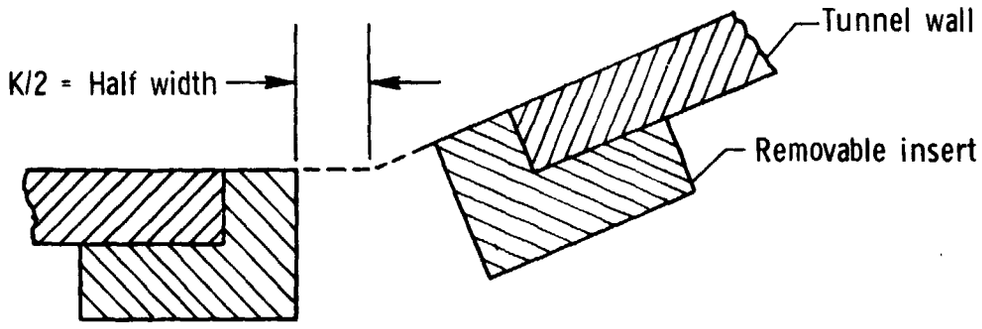

Cross section at station S
(See figure .11 for definition of S)

Station S, cm	K/2, cm
17.145	0
18.250	0
19.357	.0274
20.462	.0516
21.569	.0706
22.674	.0876
23.782	.1013
24.886	.1133
25.994	.1242
27.099	.1328
28.207	.1402
29.312	.1476
30.419	.1529
31.524	.1585
32.631	.1631
33.736	.1679
34.844	.1704
35.949	.1737
37.056	.1770
38.161	.1798

Station S, cm	K/2, cm
39.268	.1826
40.373	.1854
41.481	↓
42.586	.1887
43.693	.1913
44.798	.1976
45.905	.2027
47.010	.2195
48.118	.2433
49.223	.2731
50.328	.3117
51.435	.3541
52.540	.4011
53.647	.4516
54.752	.5034
55.860	.5530
56.965	.6055
58.072	.6513
59.177	.6988
60.284	.7468

Station S, cm	K/2, cm
61.389	.7915
62.497	.8324
63.602	.8679
64.707	.8997
65.814	.9263
66.921	.9495
68.026	.9347
↓	↓
↓	↓
102.870	↓

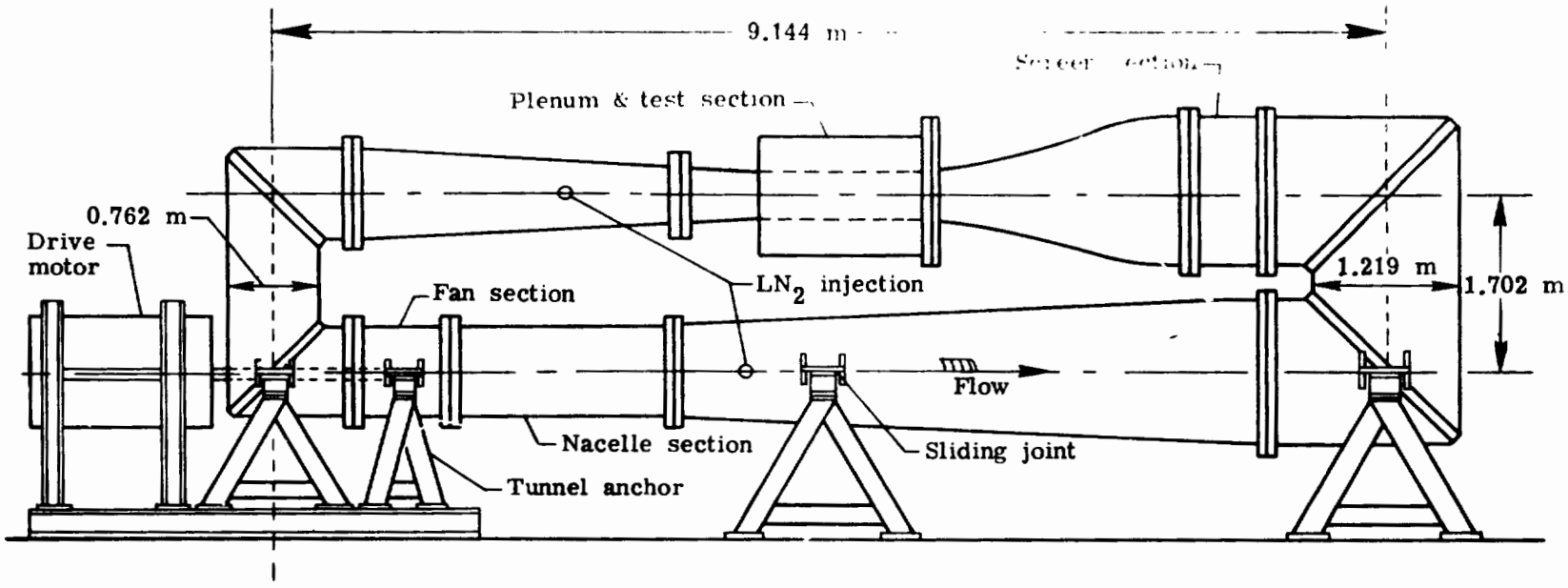

Figure 1.- Layout of transonic cryogenic tunnel circuit.

Figure 2.- Transonic cryogenic tunnel during assembly.

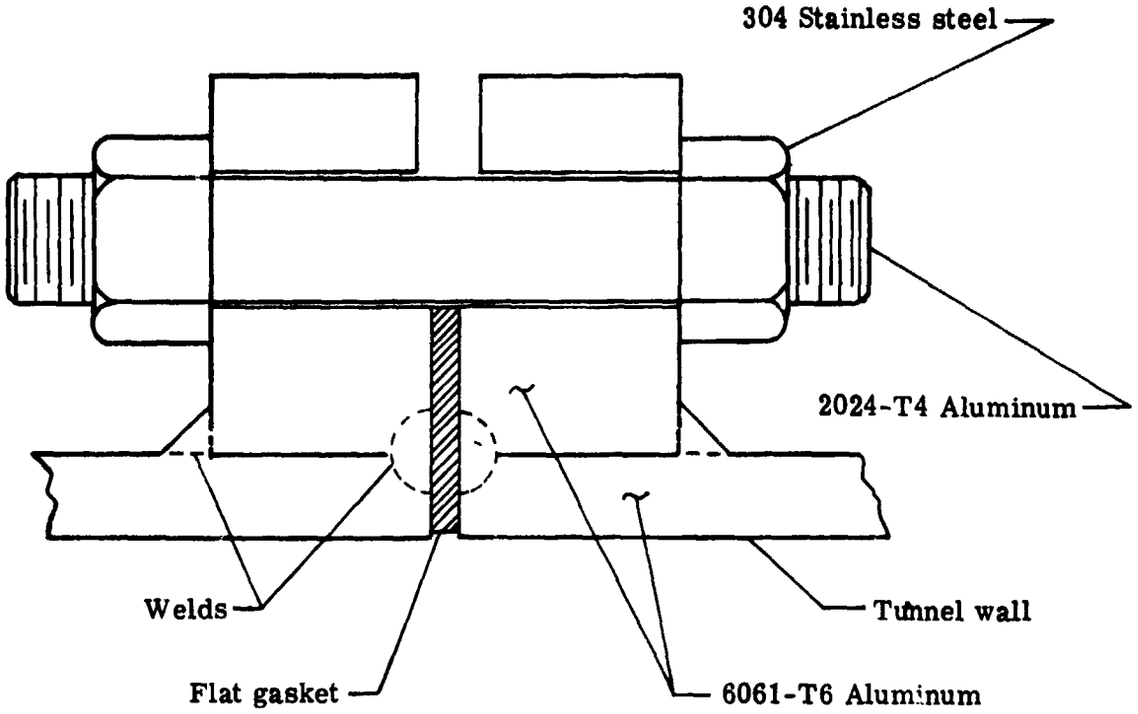

a) Typical small flange joint with flat gasket seal

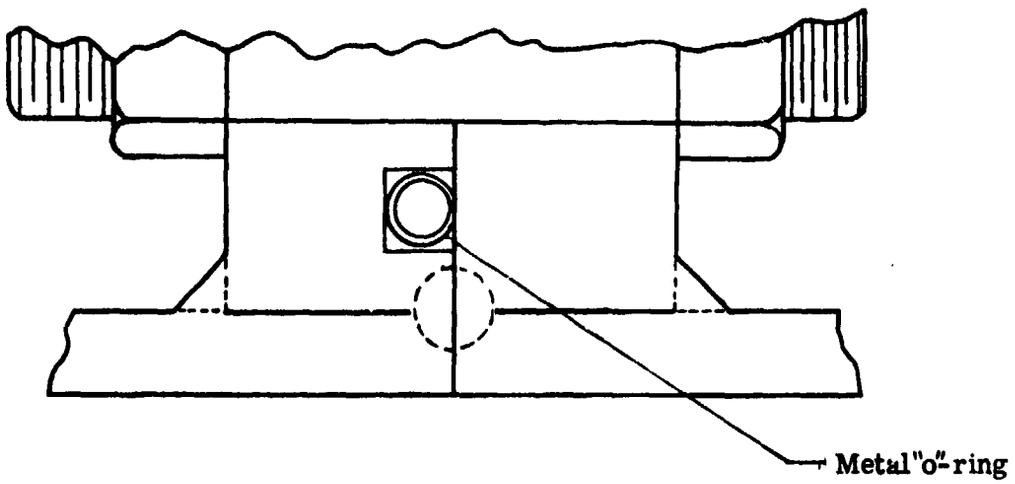

b) Typical large flange joint with teflon coated metal "o"-ring seal

Figure ~ - Typical flange joints showing details of seals.

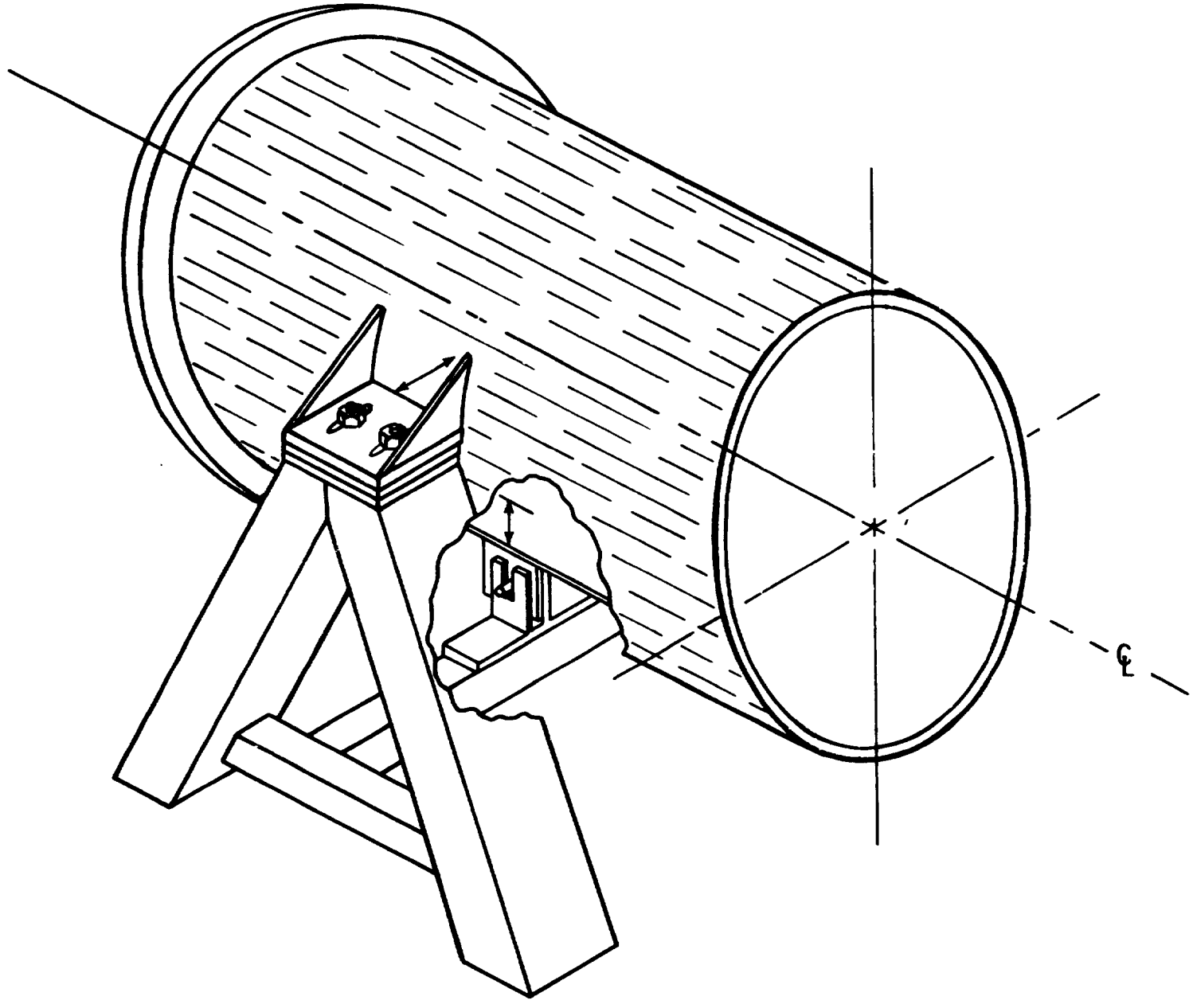

Figure 4.- Transonic cryogenic tunnel anchor support.

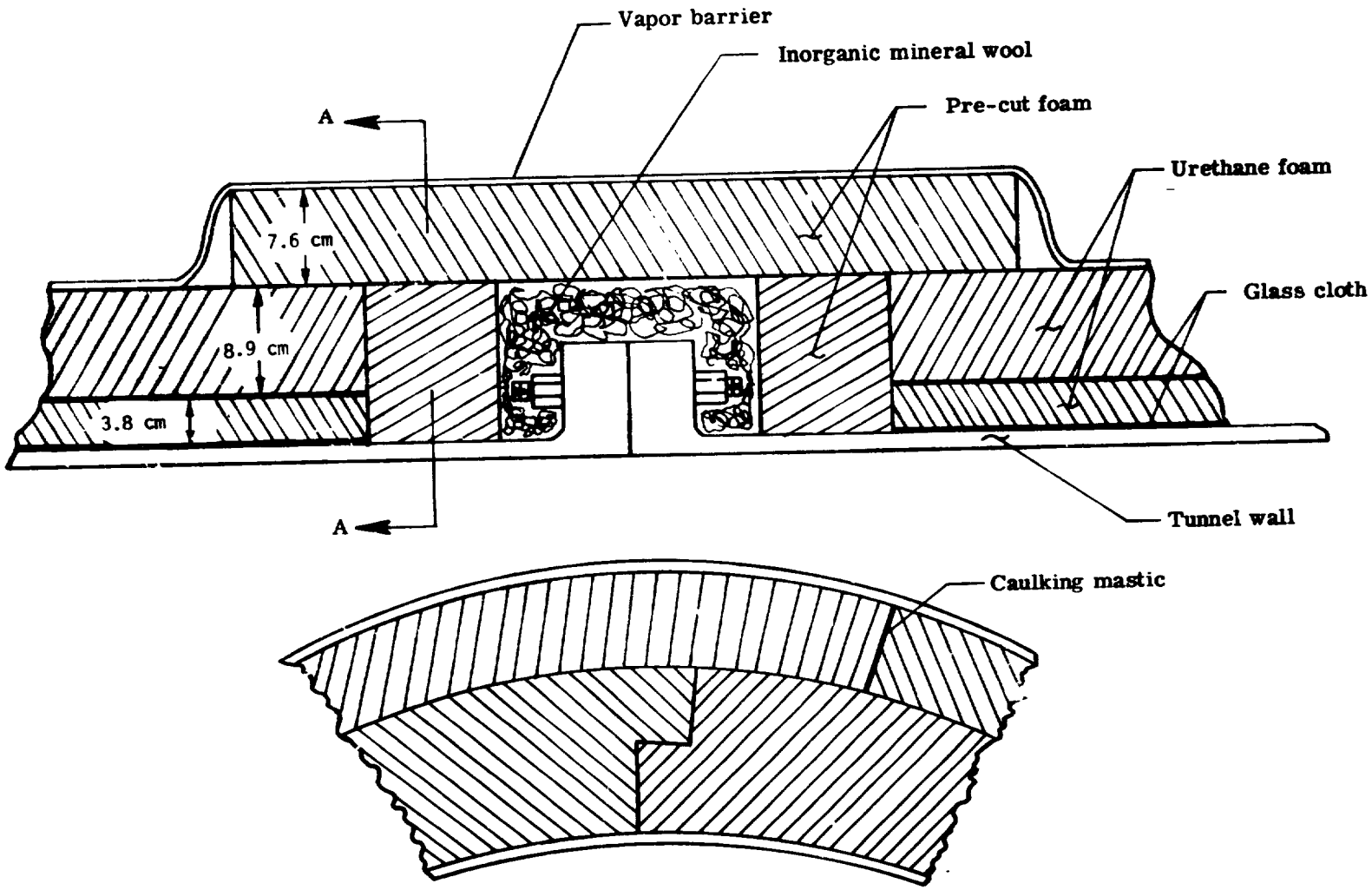

Figure 5.- Details of insulation used on transonic cryogenic tunnel.

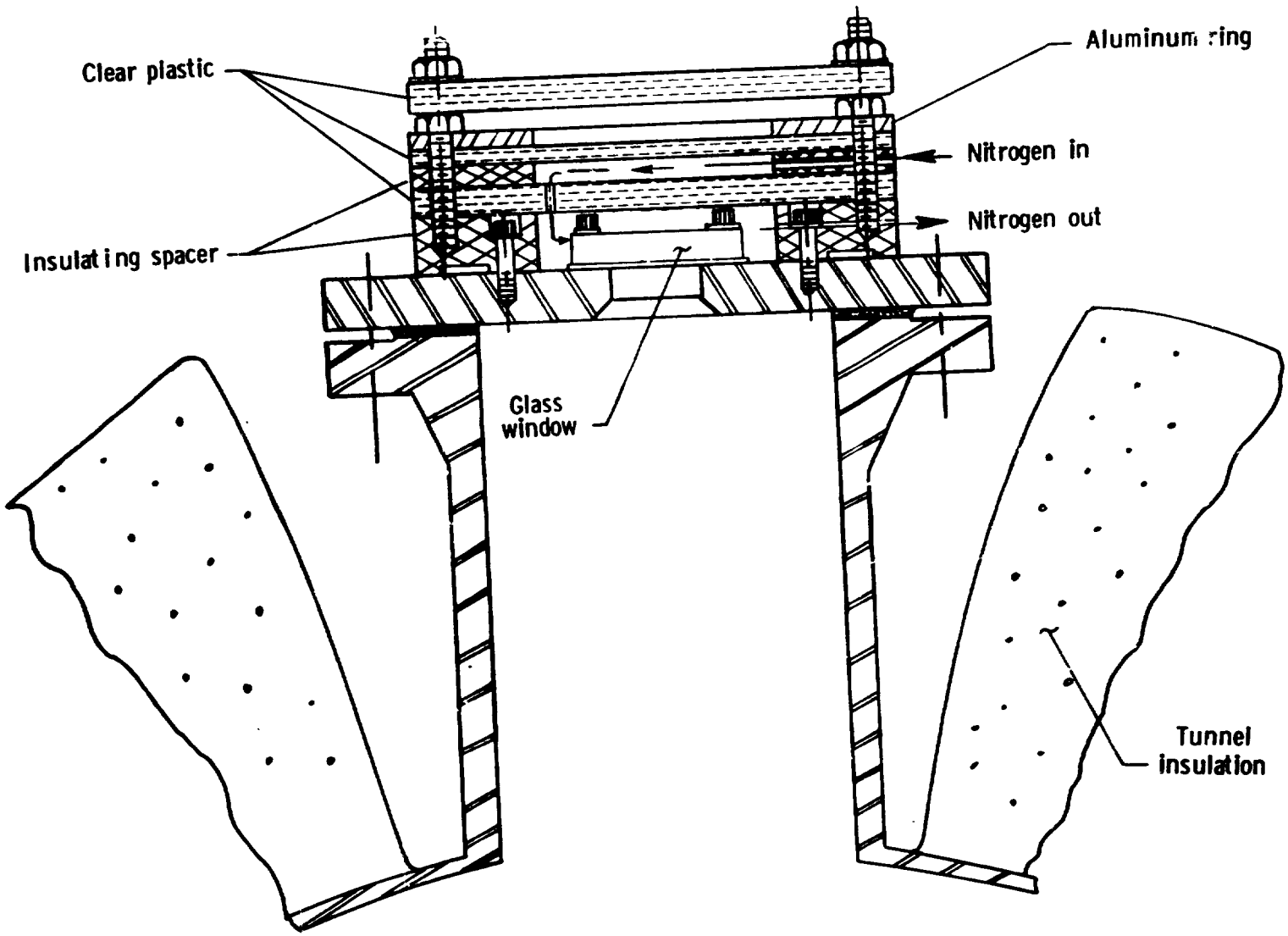

Figure 6.- Transonic cryogenic tunnel port.

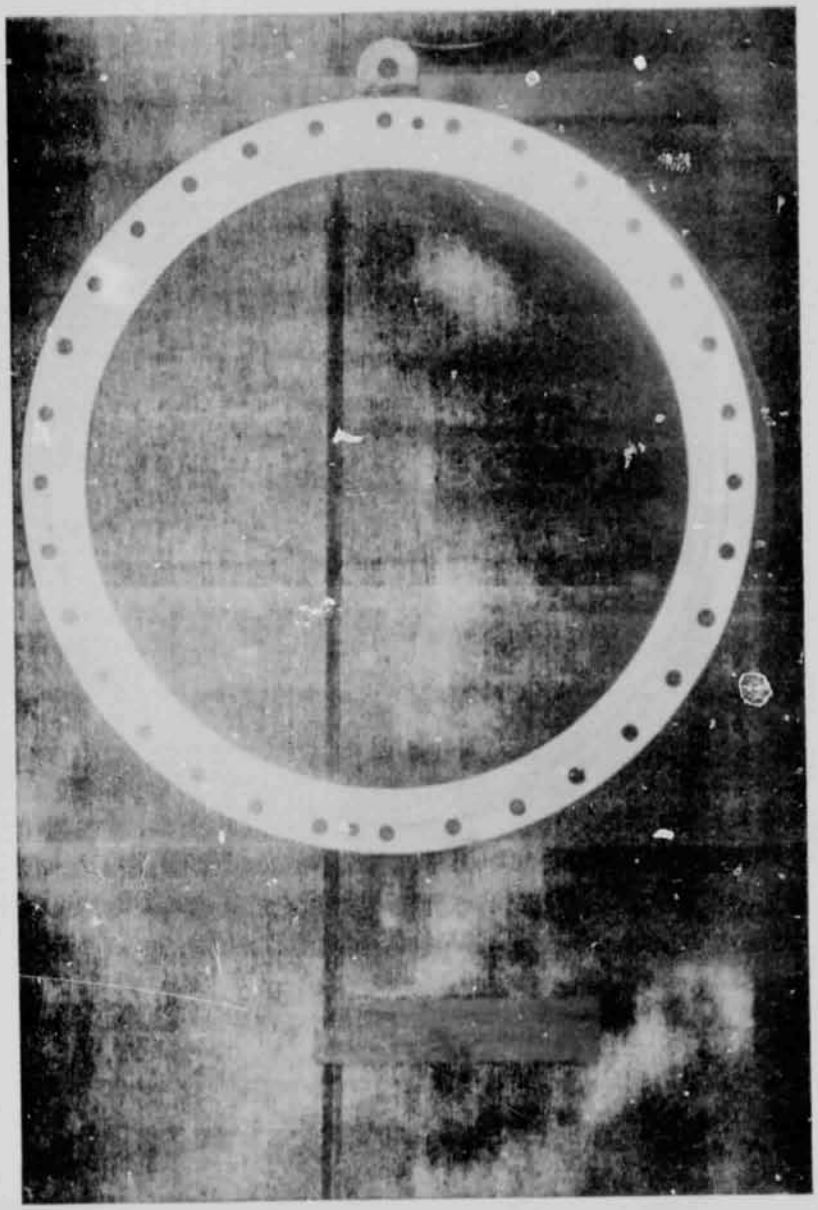

Figure 7.- View looking upstream showing the nacelle section and fan section.

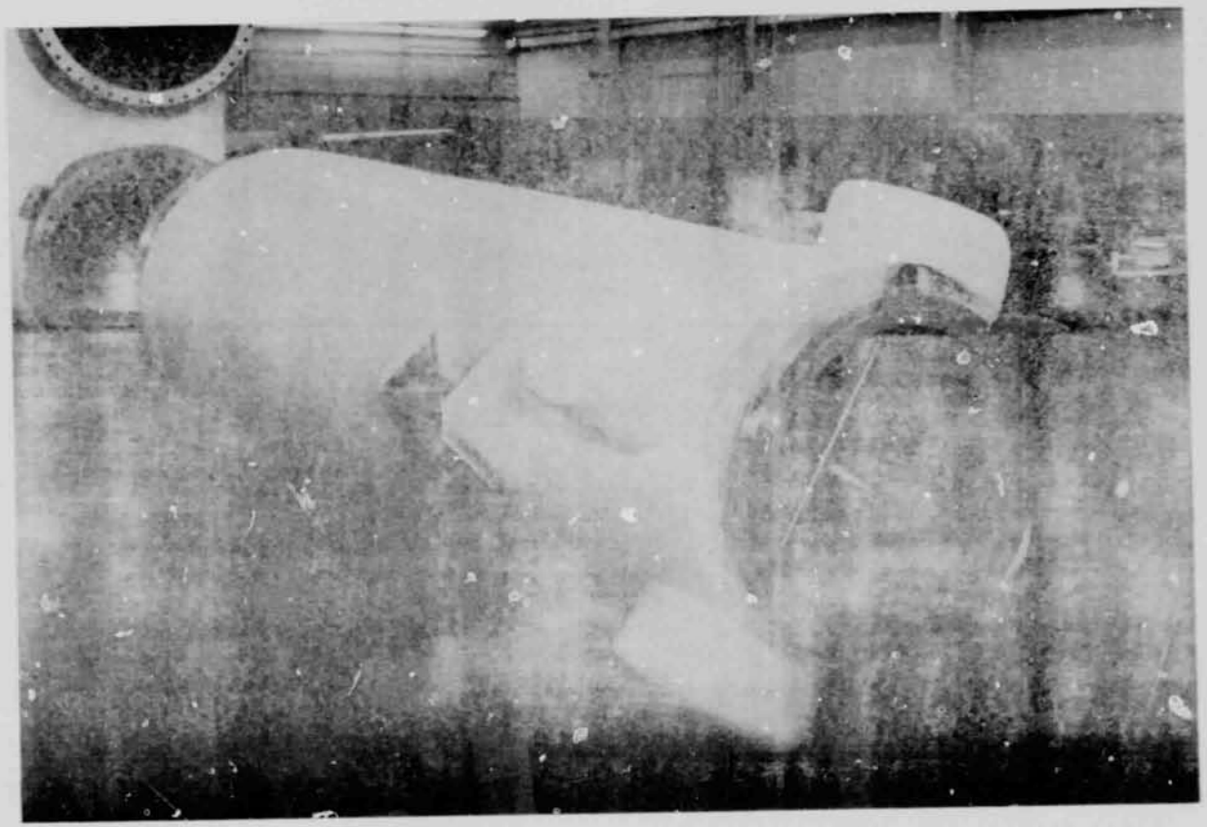

Figure 8.- Return-leg diffuser and third and fourth corners.

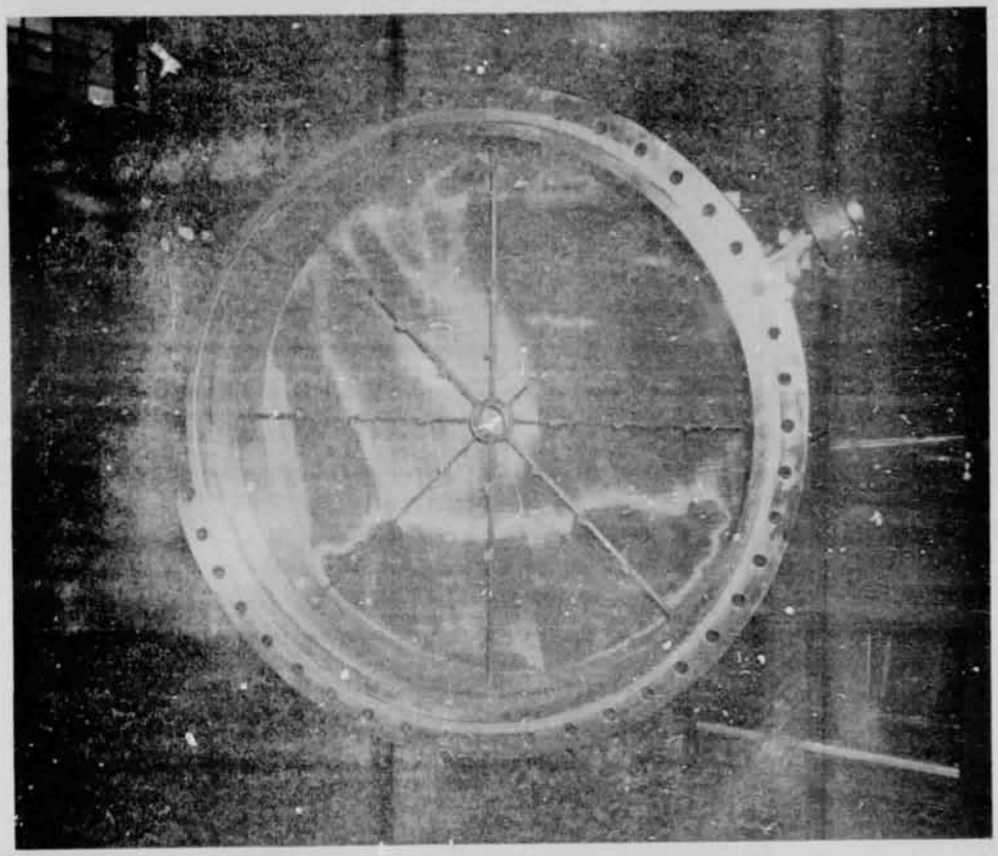

Figure 9.- Screen section showing the temperature survey rig.

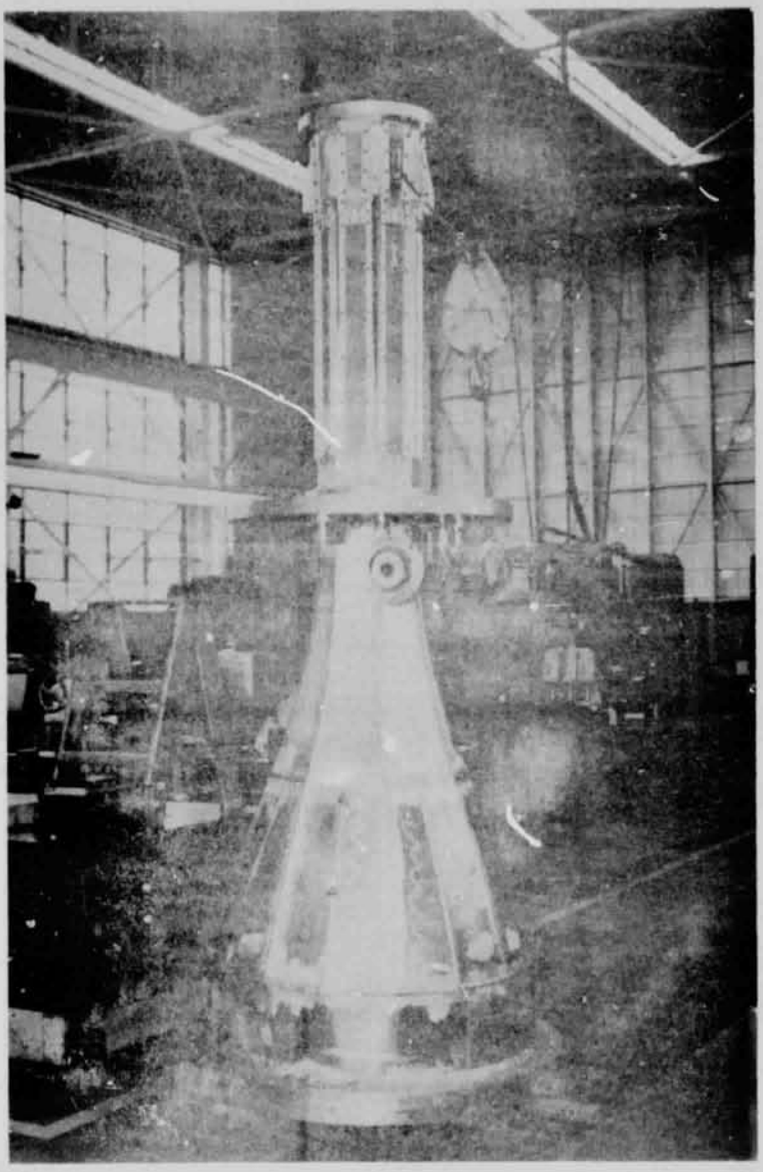

Figure 10.- Contraction section and test section.

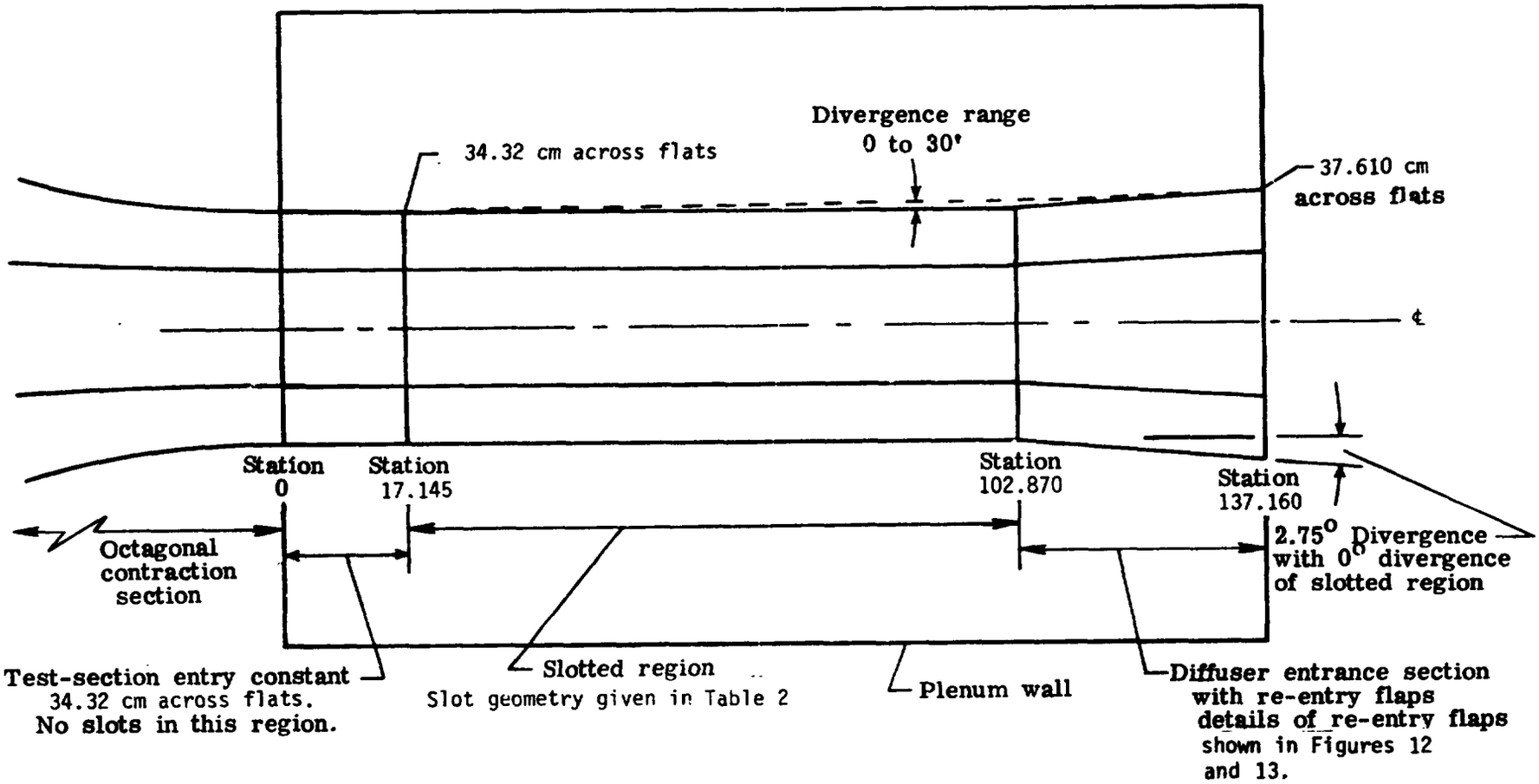

Figure 11.- Layout of test section. Station given in centimeters. Wall divergence set at 5' for initial tests.

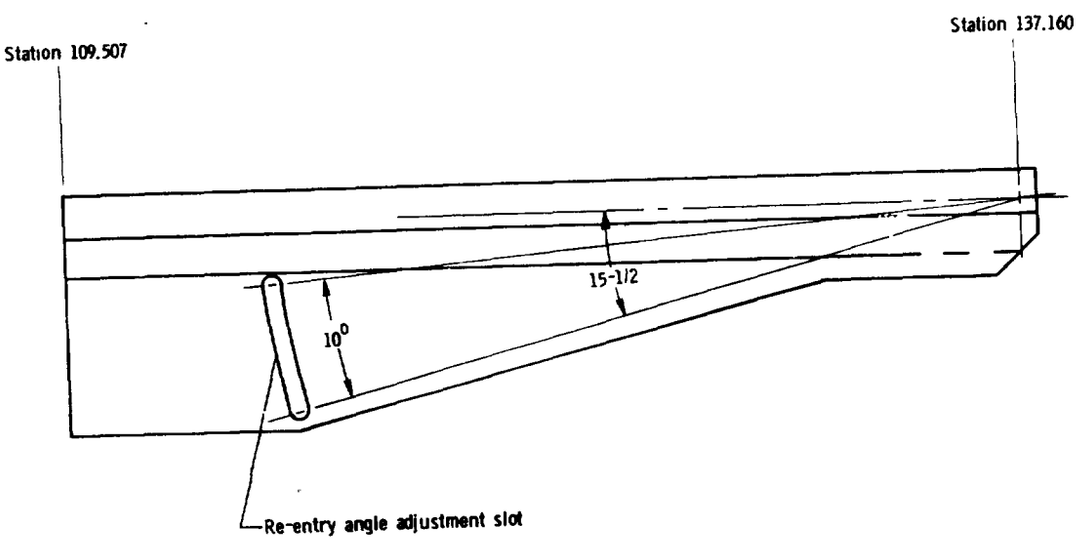

Side view of side plate

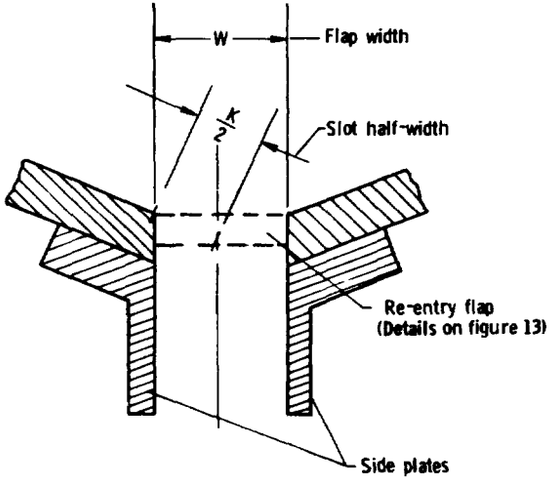

S, cm	K/2, cm
109.507	1.472
110.338	1.489
111.719	1.516
116.144	1.605
120.569	1.693
124.993	1.781
129.418	1.869
137.160	2.023

Figure 12.- Details of re-entry slot design. Re-entry flap set at 7° for initial tests.

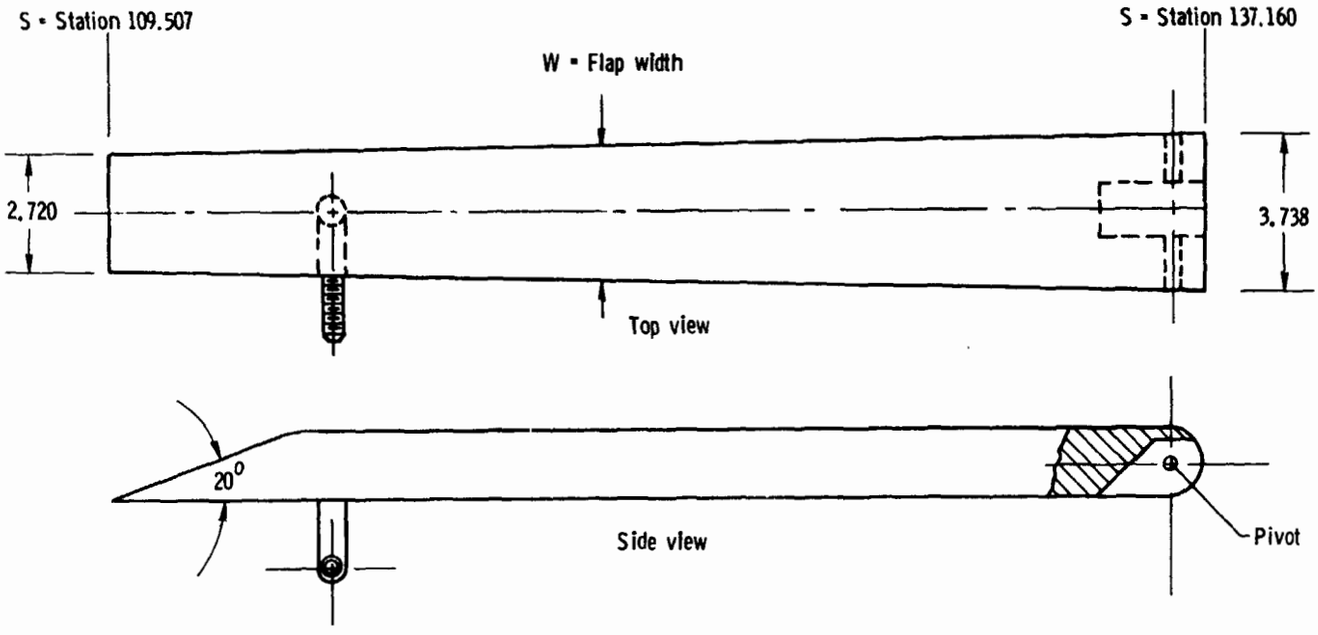

S, cm	W, cm
109.507	2.720
110.338	2.751
111.719	2.802
116.144	2.967
120.569	3.128
124.993	3.291
129.418	3.453
137.160	3.738

Figure 13.- Details of re-entry flap design.

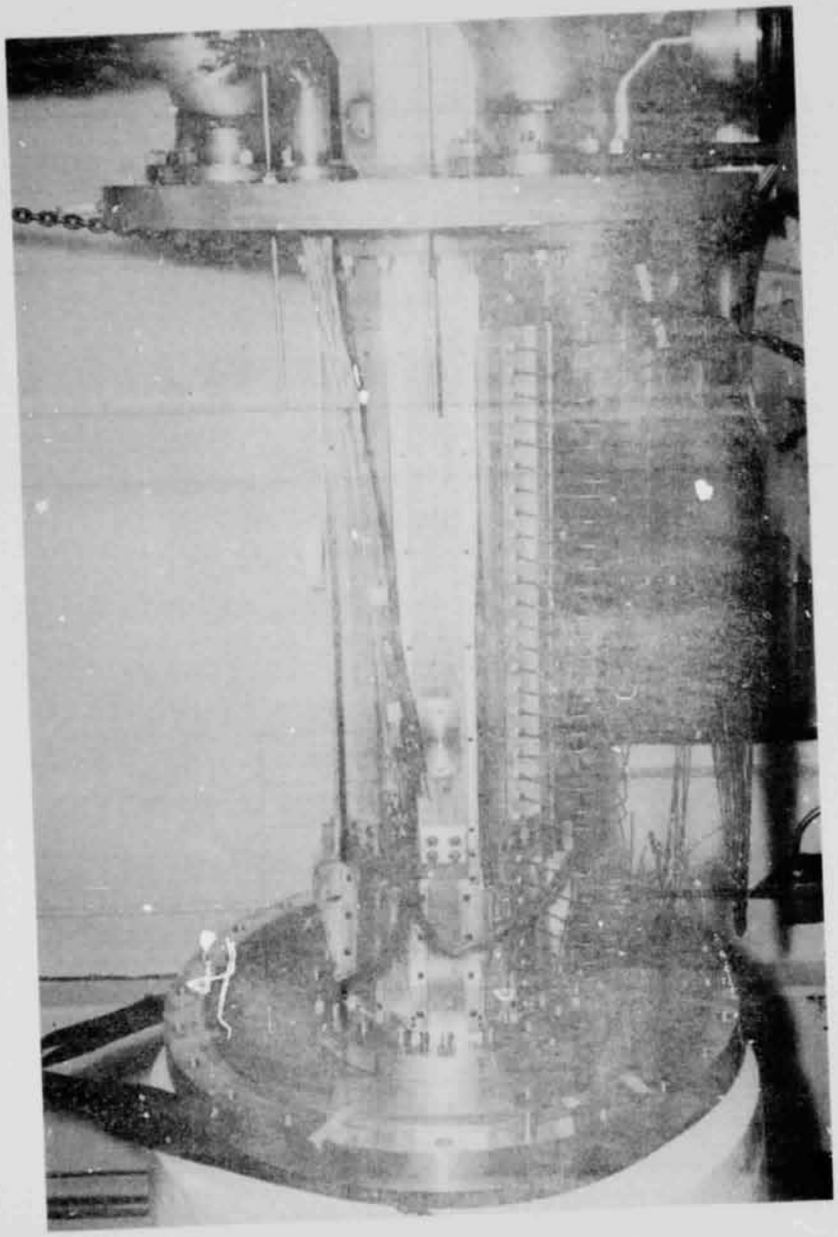

Figure 14.- Transonic cryogenic tunnel test section.

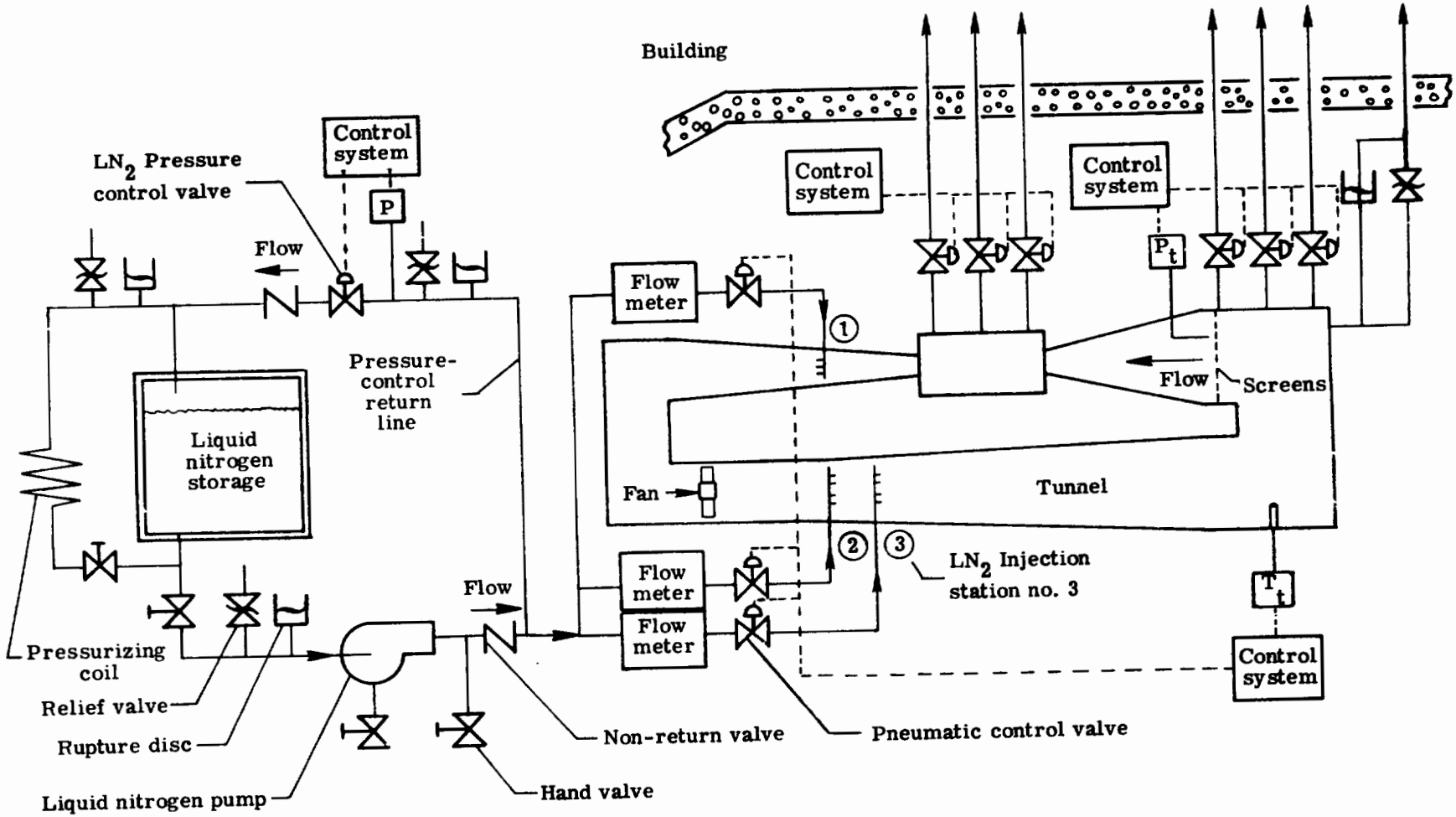

Figure 15.- Schematic drawing of the liquid nitrogen system and nitrogen exhaust system.

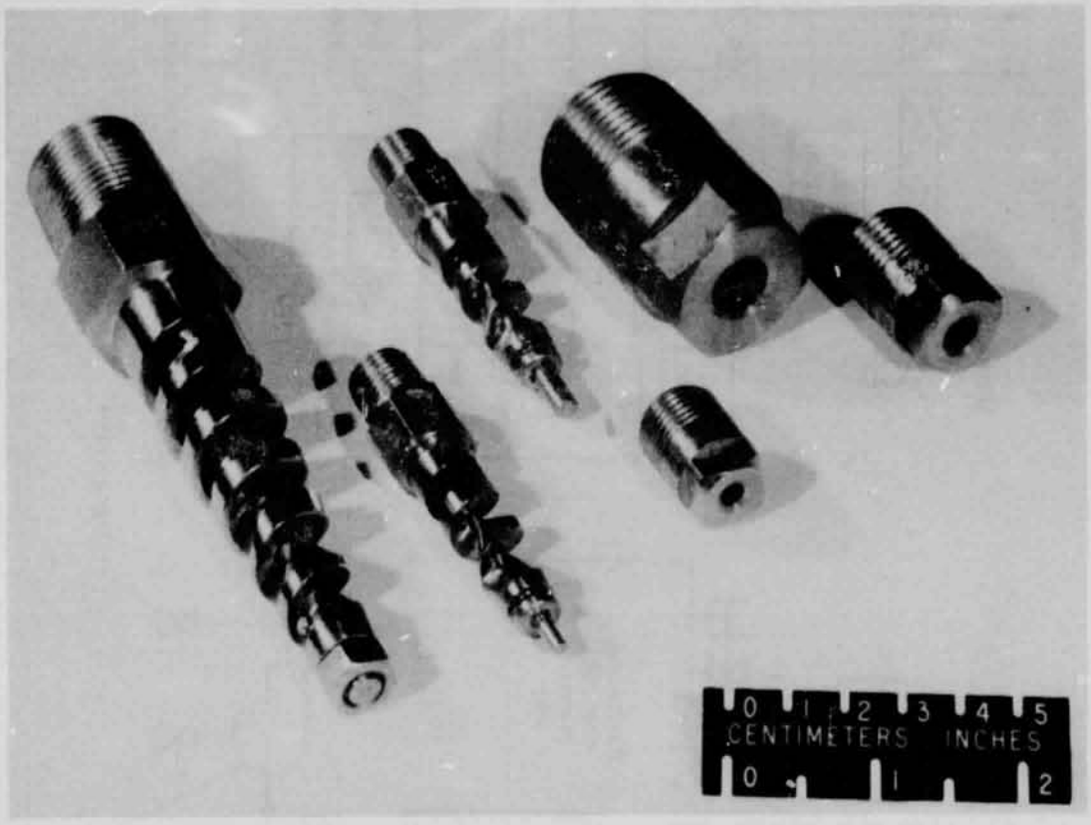

Figure 16.- Liquid-nitrogen injection nozzles.

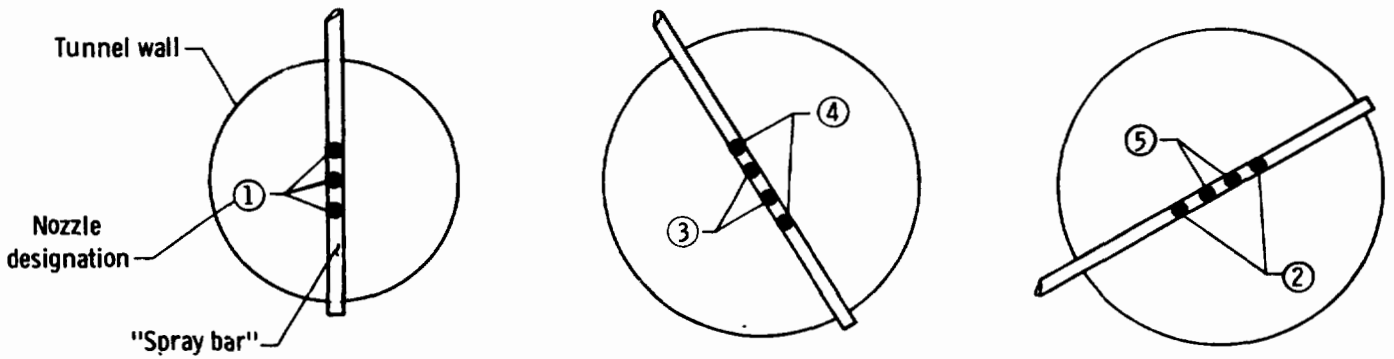

Nozzle designation	Manufacturers model number	Liquid nitrogen flow rate liter per minute at stated differential pressure								
		0.5 atm	1 atm	2 atm	3 atm	4 atm	5 atm	6 atm	7 atm	8 atm
1†	1HH12	51.4	72.5	98.2	118.4	135.2	149.6	163.0	175.7	187.5
2	1/2HHSS4.0	13.9	20.0	27.8	33.5	38.3	42.8	46.8	50.4	53.7
3	3/8HHSS9.5	3.41	4.97	6.74	8.00	9.14	10.15	11.04	11.92	12.68
4	AA6FC	2.49	3.83	5.56	6.74	7.88	8.59	9.27	9.72	10.20
5	B16FC	19.0	27.0	38.3	46.8	53.9	60.3	66.1	71.2	76.0

† Nozzles 1, 2, and 3 were manufactured by Spraying Systems Co., Wheaton, Ill., U.S.A.
Nozzles 4 and 5 were manufactured by Bete Fog Nozzle, Inc., Greenfield, Mass., U.S.A.

Figure 17.- Sketches of the three liquid nitrogen spray bars with tabulated flow capacity for each type nozzle.

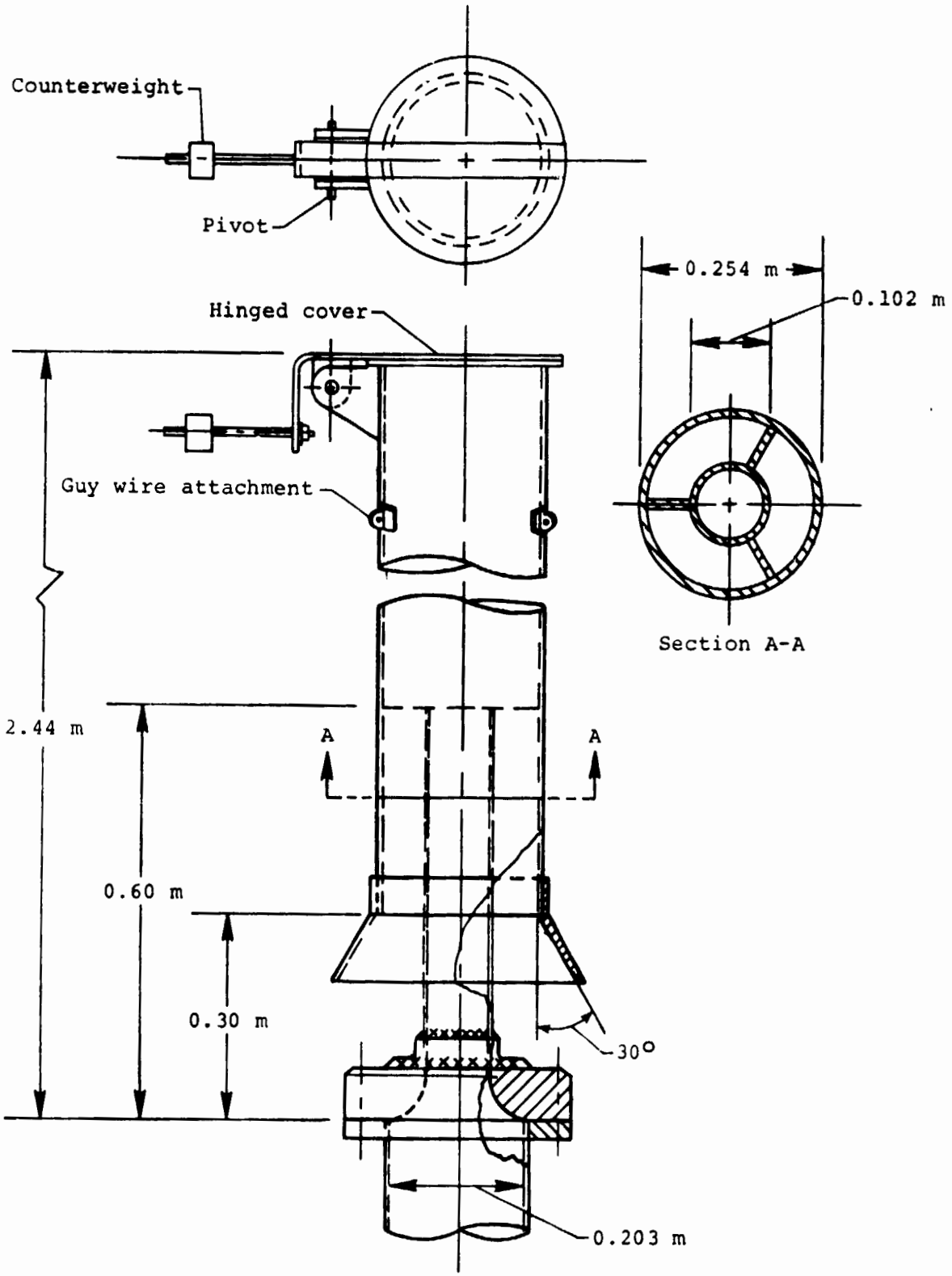

Figure 18.- Tunnel exhaust ejector.

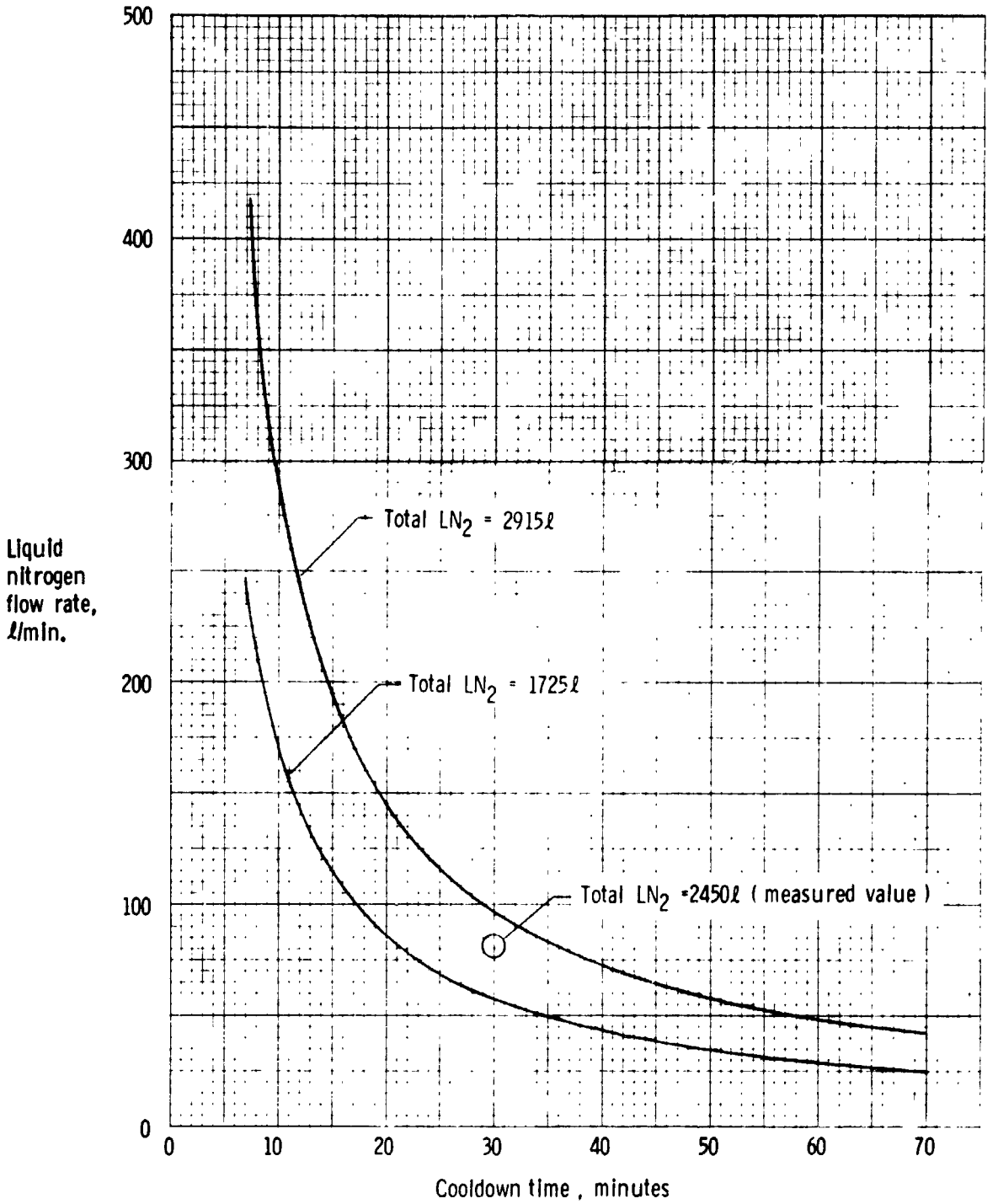

Figure 19.- Required liquid nitrogen flow rate as a function of cooldown time for cooling the transonic tunnel from 300 K to 110 K.

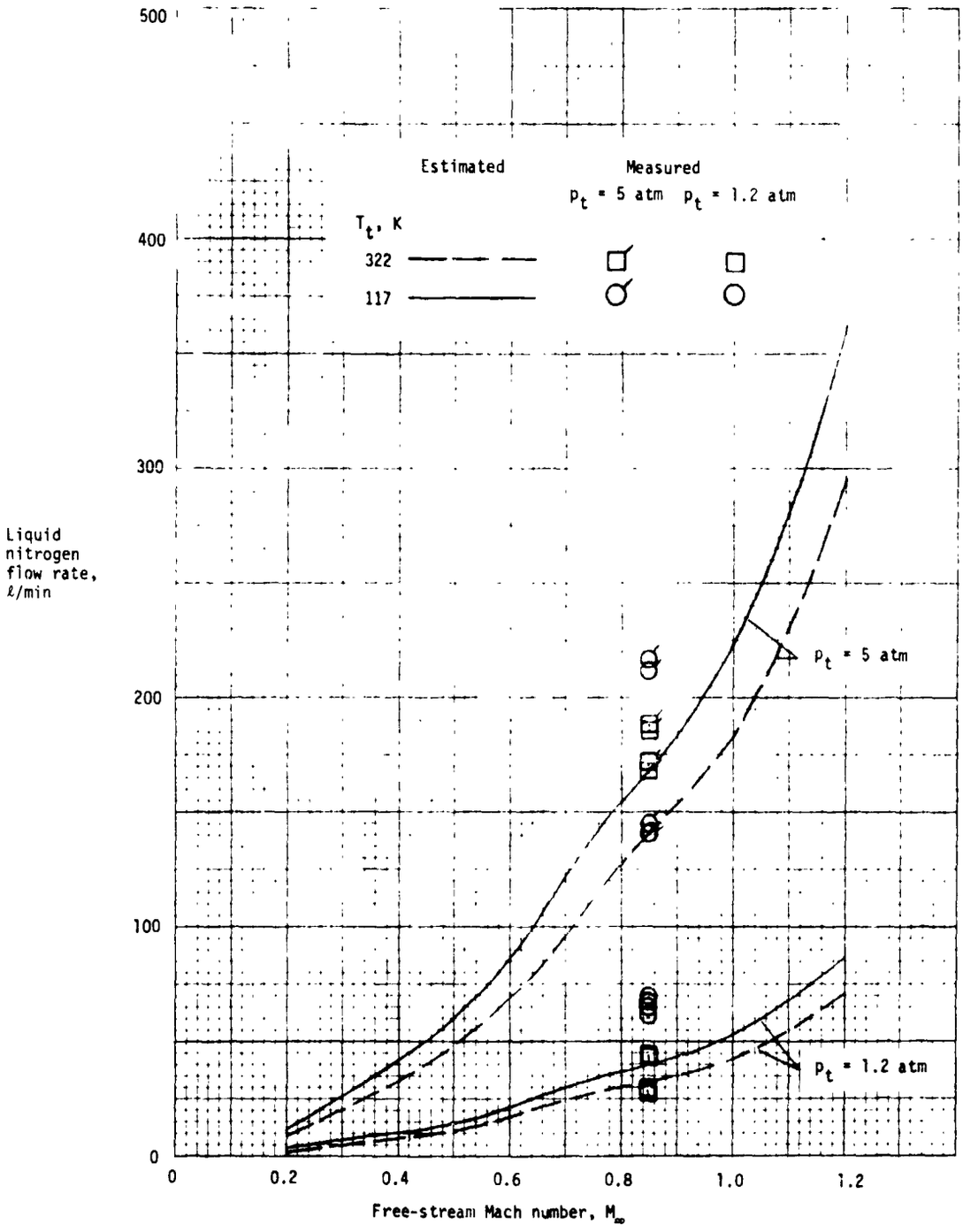

Figure 20.- Required liquid nitrogen flow rate as a function of test Mach number, pressure, and temperature.

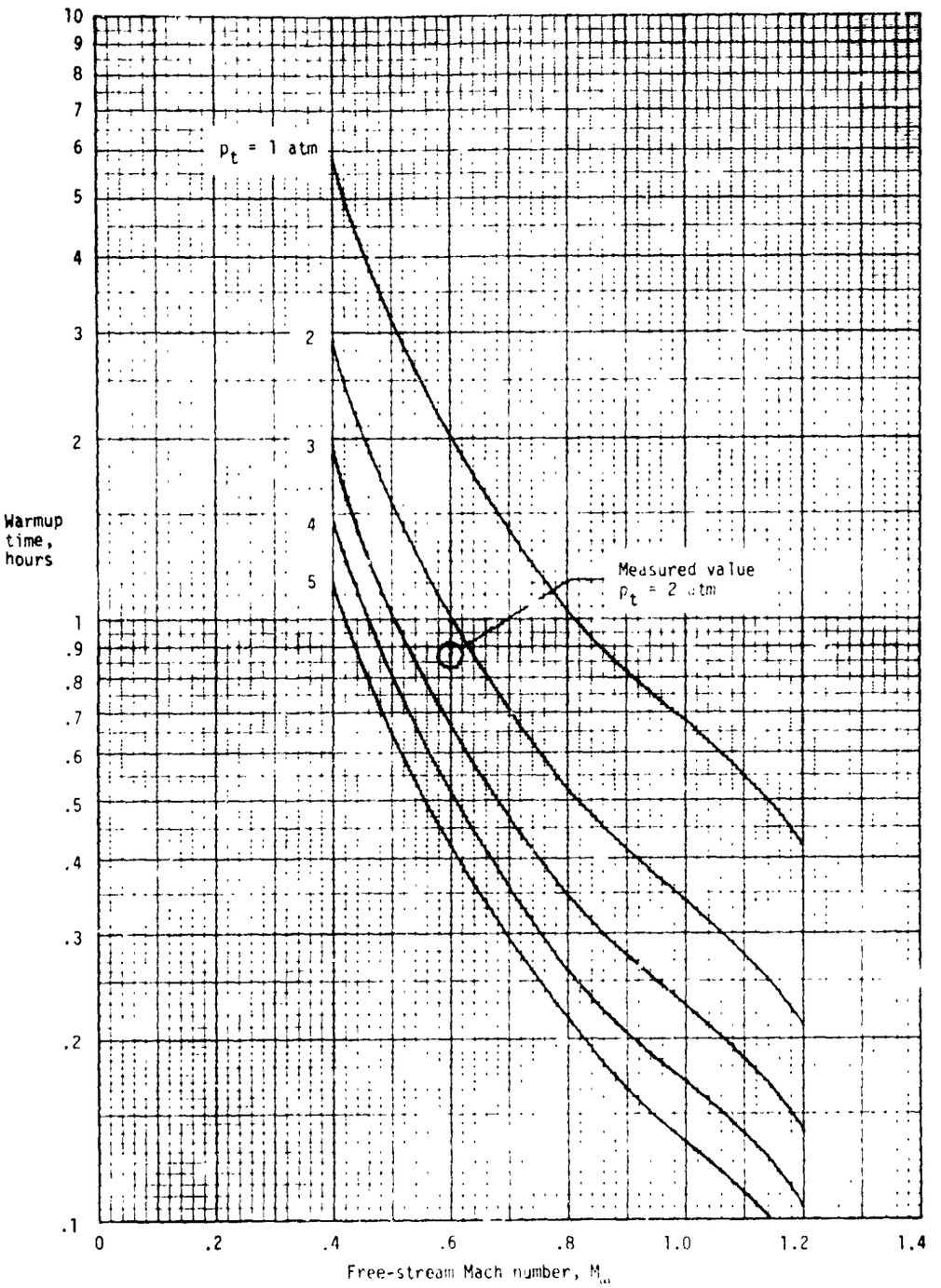

Figure 21.- Warm-up time as a function of Mach number and pressure for warming the transonic tunnel from 110 K to 300 K.

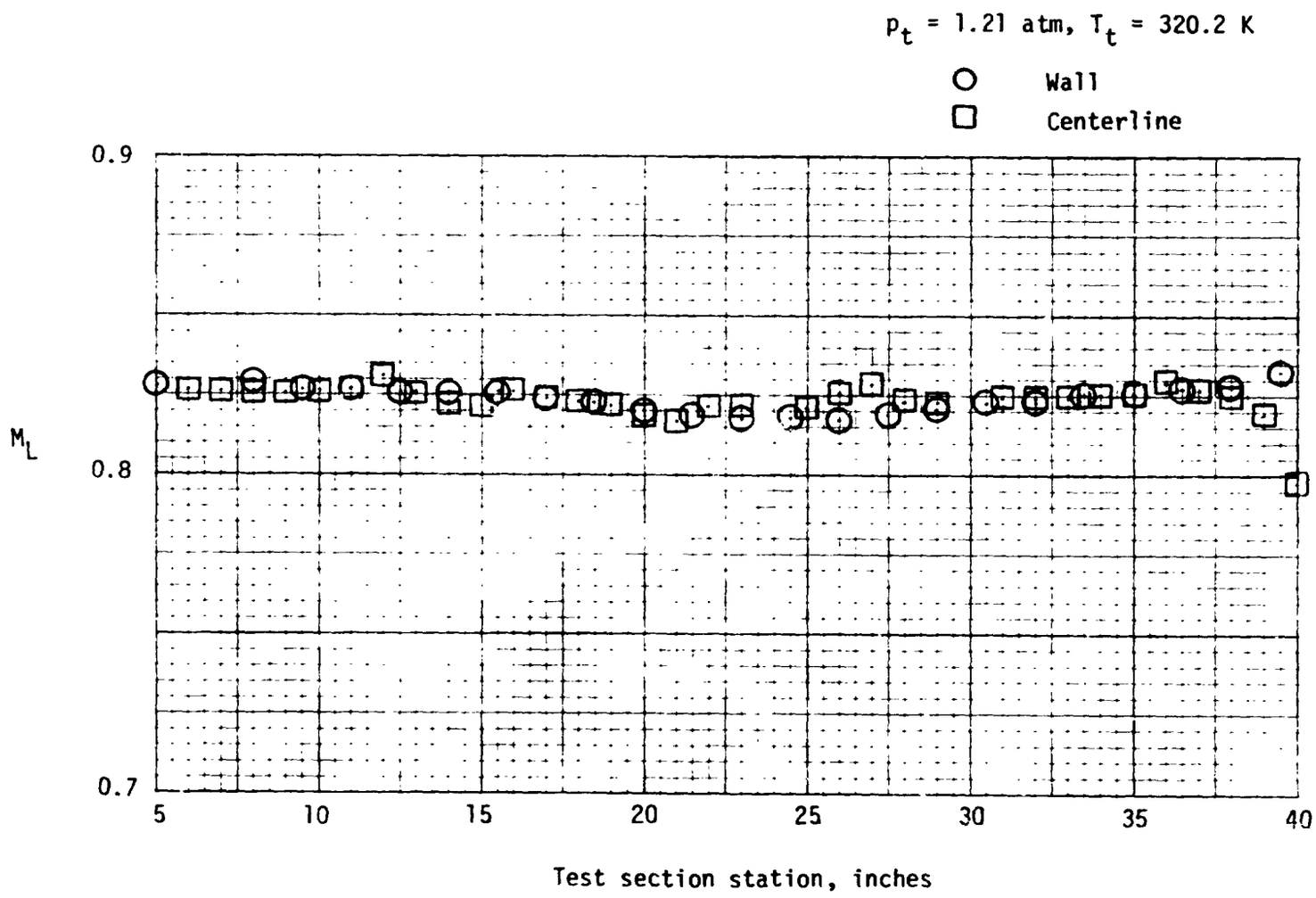

Figure 22.- Examples of test-section wall and centerline Mach number distribution at $M_\infty \approx 0.825$.

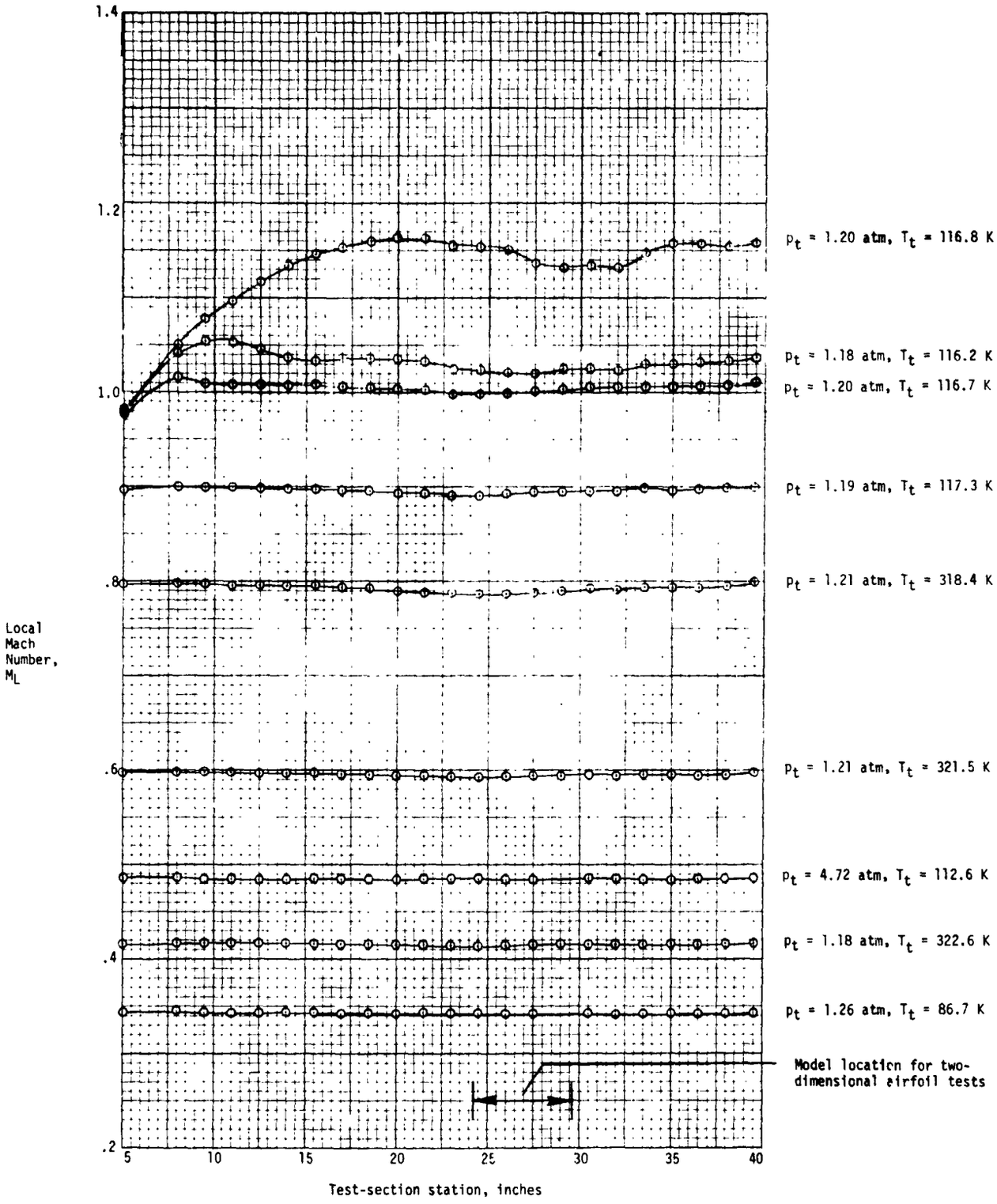

Figure 23.- Examples of test-section wall Mach number distribution for several values of Mach number.

M_∞ = 0.85

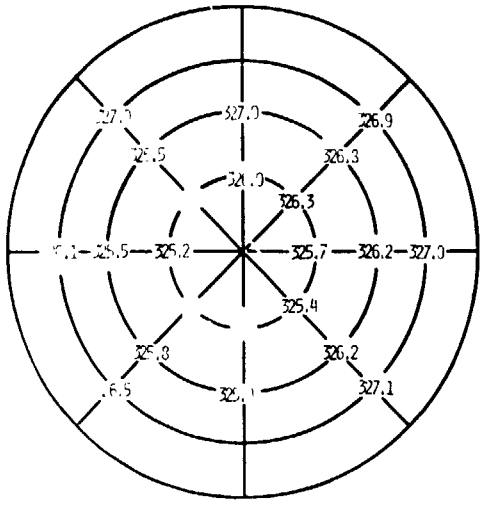

T_t = 326.3 K, σ = 0.6 K

p_t = 5 Atm.

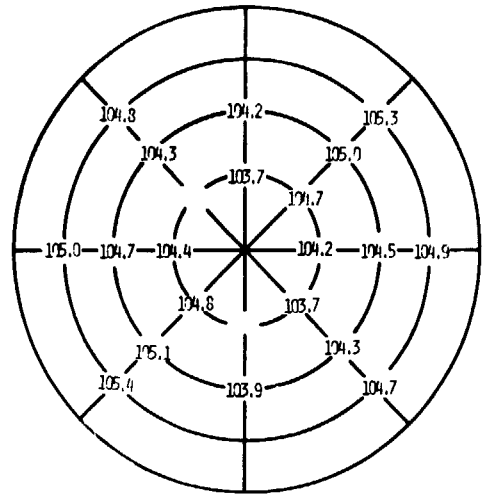

T_t = 104.6 K, σ = 0.5 K

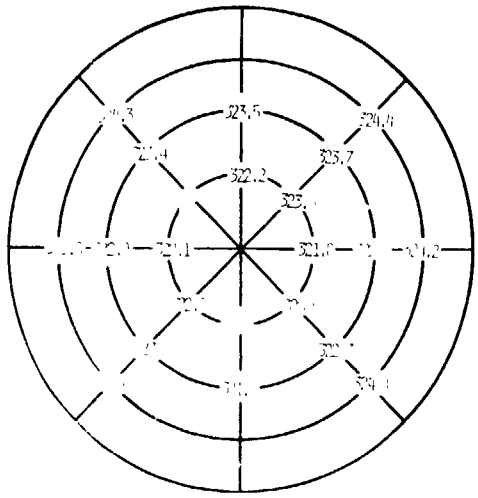

T_t = 323.1 K, σ = 1.0 K

p_t = 2.5 Atm.

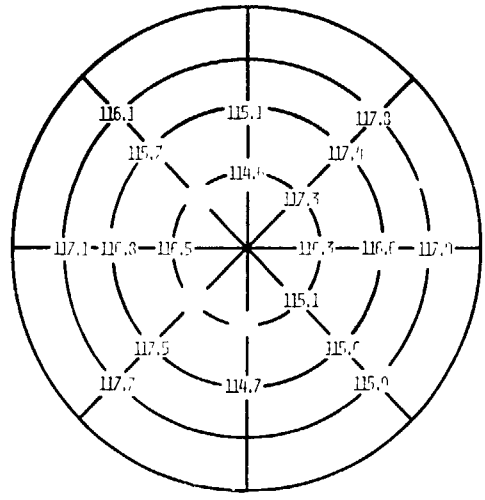

T_t = 116.4 K, σ = 1.0 K

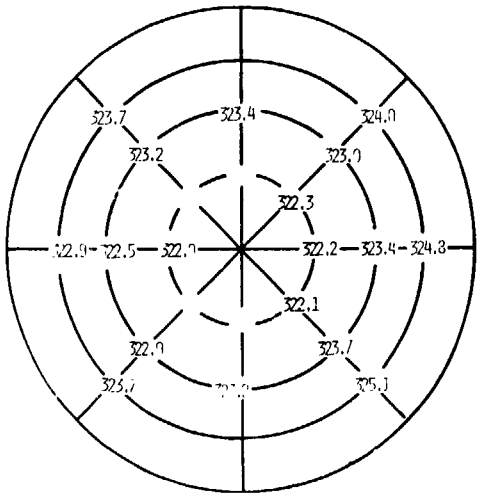

T_t = 323.2 K, σ = 0.9 K

p_t = 1.2 Atm.

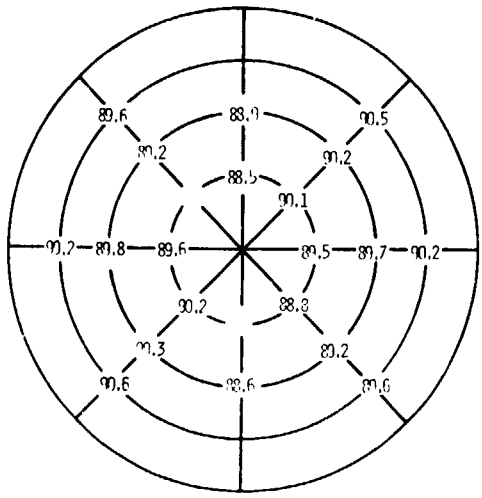

T_t = 89.7 K, σ = 0.6 K

Figure 24.- Examples of transverse temperature distribution in the transonic cryogenic tunnel. Measurements made upstream of the screens.

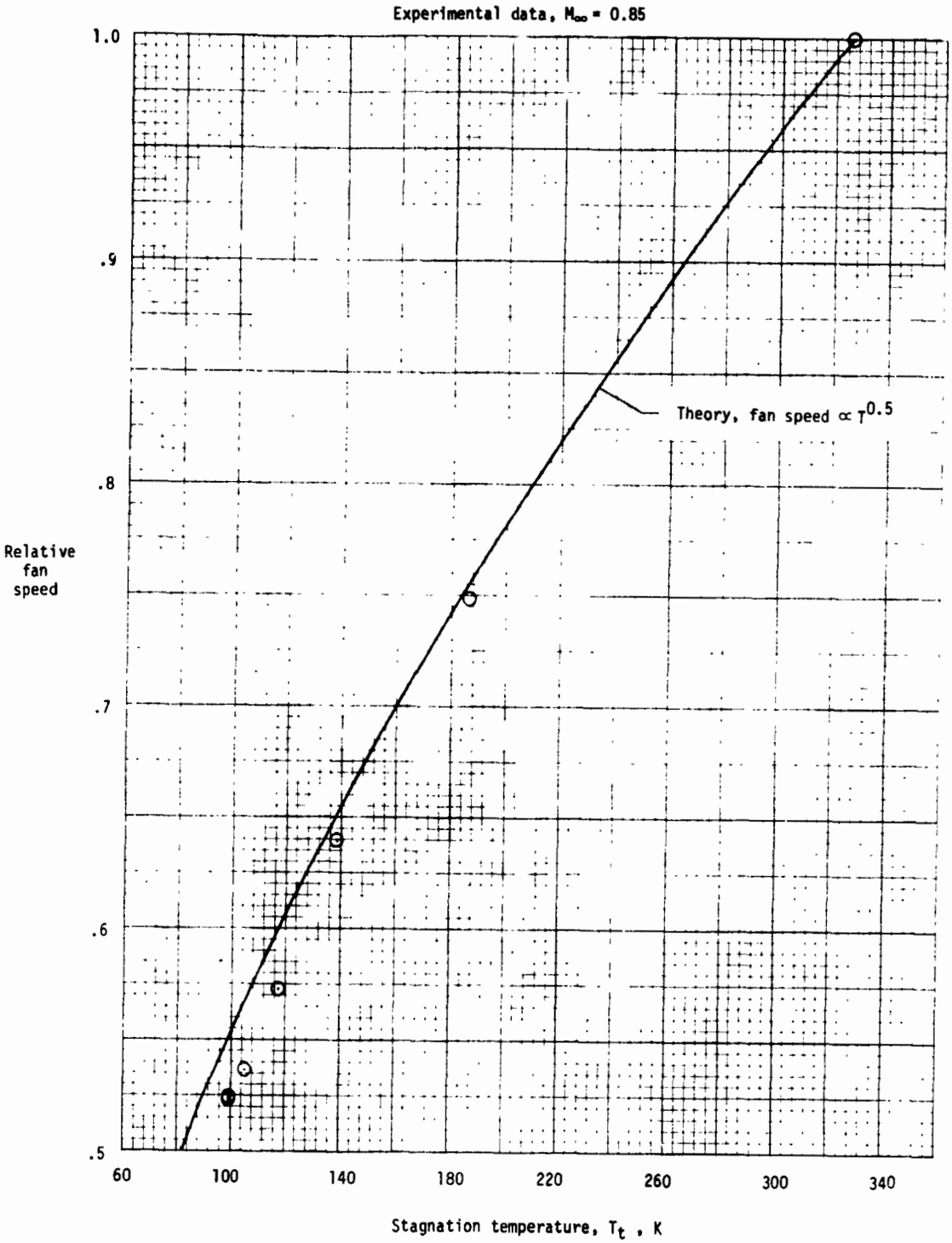

Figure 25.- Theoretical and measured variation of fan speed relative to maximum fan speed with stagnation temperature at $M_\infty = 0.85$.

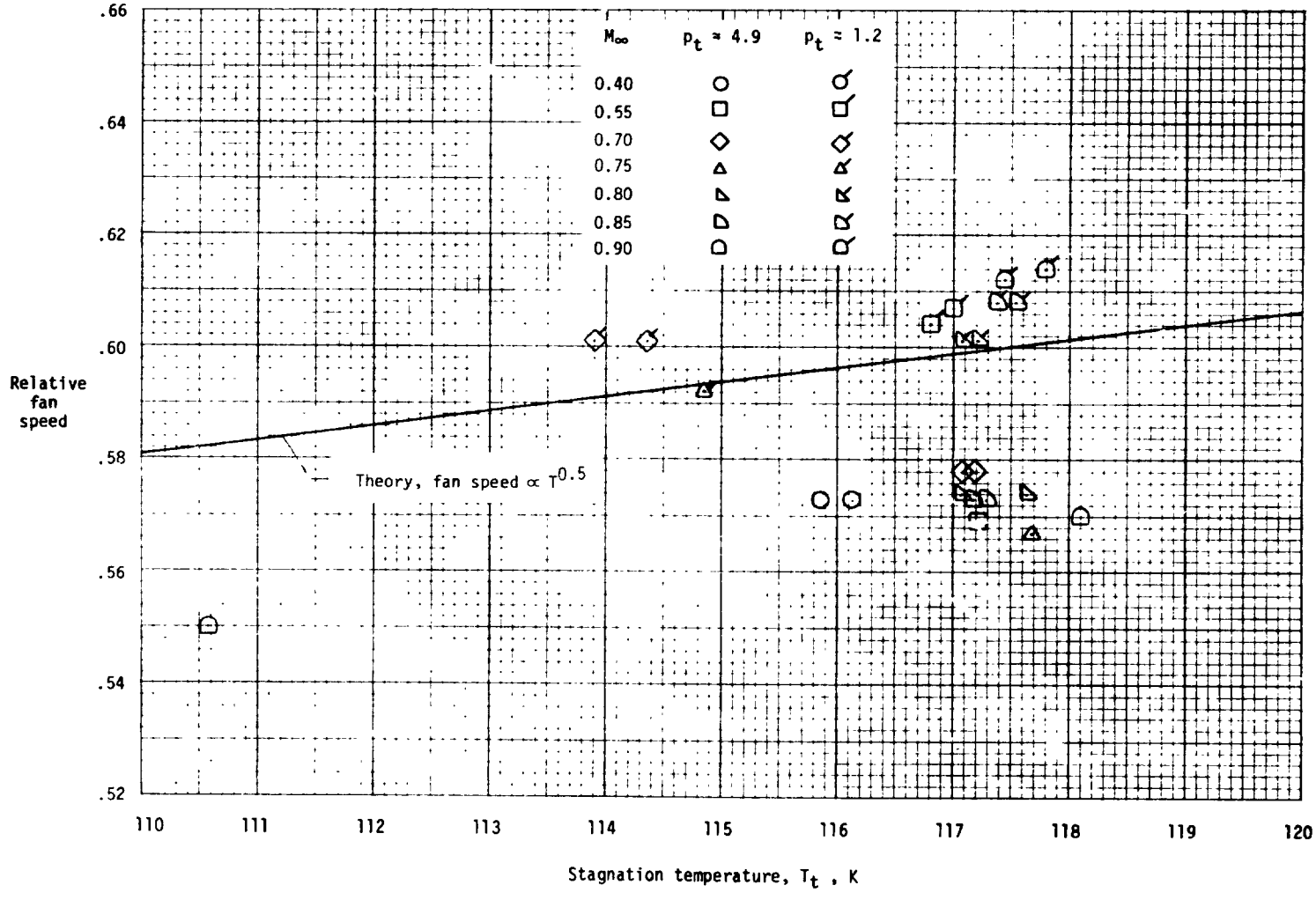

Figure 26.- Theoretical and measured variation of fan speed relative to maximum fan speed with stagnation temperature for several values of Mach number.

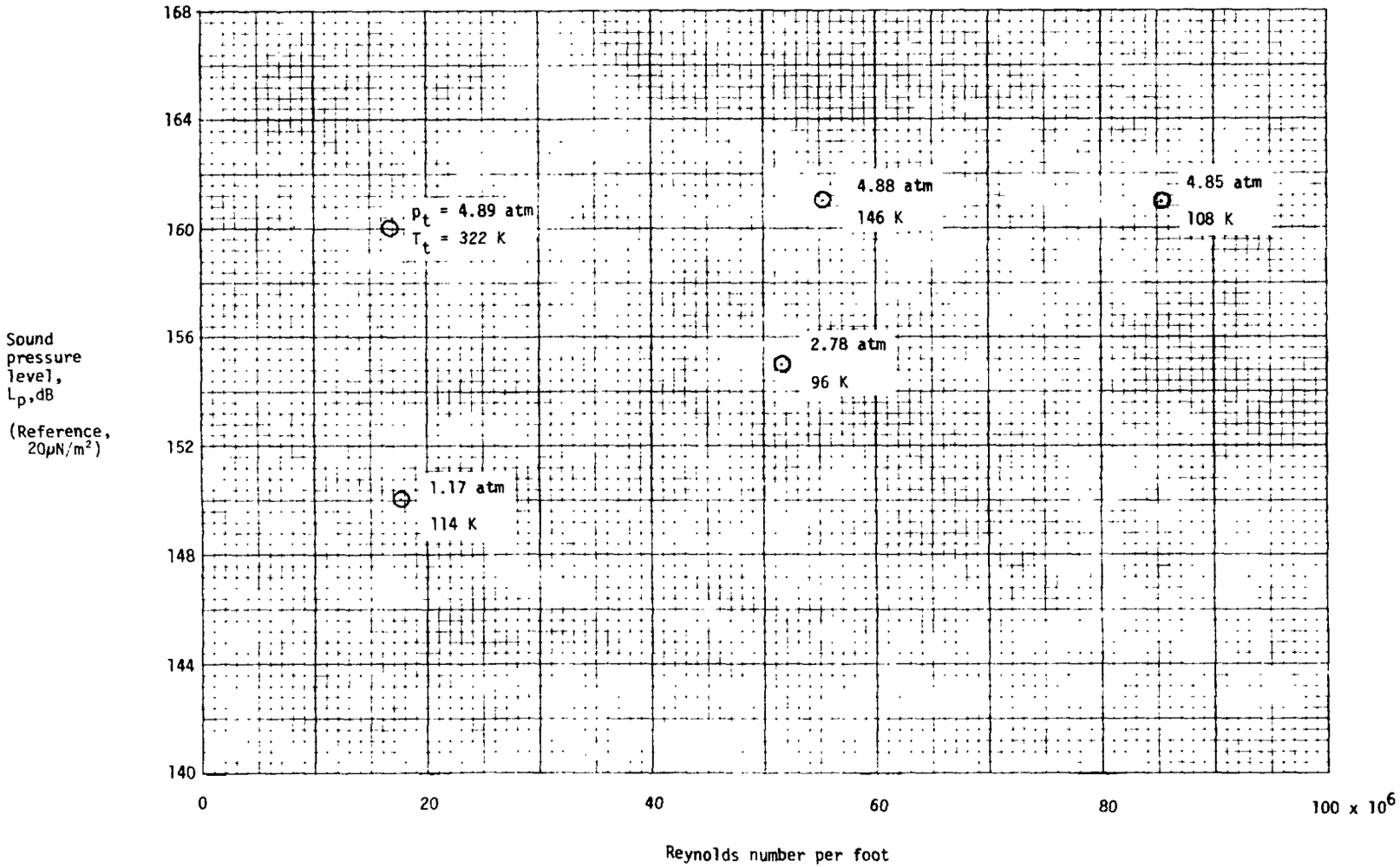

Figure 27.- Broadband sound pressure level in the test section as a function of Reynolds number for various combinations of temperature and pressure at $M_\infty = 0.80$.